UC Berkeley

Title

A field theory approach to the statistical kinematic dynamo

Permalink

Journal

ISSN

Authors

Holdenried-Chernoff, Daria
King, David A
Buffett, Bruce A

Publication Date

DOI

Copyright Information

Peer reviewed

A field theory approach to the statistical kinematic dynamo

Daria Holdenried-Chernoff,[1, *] David A. King,[2] and Bruce A. Buffett[1]

[1]*Department of Earth and Planetary Science, University of California, Berkeley*
[2]*Department of Physics and Astronomy, University of Pennsylvania, 209 South 33rd St., Philadelphia, PA, 19104.*
(Dated: January 19, 2024)

Variations in the geomagnetic field occur on a vast range of time scales, from milliseconds to millions of years. The advent of satellite measurements has allowed for detailed studies of short timescale geomagnetic field behaviour, but understanding its long timescale evolution remains challenging due to the sparsity of the paleomagnetic record. This paper introduces a field theory framework for studying magnetic field generation as a result of stochastic fluid motions. Starting from a stochastic kinematic dynamo model (the Kazantsev kinematic model), we derive statistical properties of the magnetic field that may be compared to observations from the paleomagnetic record. The fluid velocity is taken to be a Kraichnan field with general covariance, which acts as a random forcing obeying Gaussian statistics. Using the Martin-Siggia-Rose-Janssen-de Dominicis (MSRJD) formalism, we compute the average magnetic field response function for fluid velocities with short correlation time. From this we obtain an estimate for the turbulent contribution to the magnetic diffusivity, and find that it is consistent with results from mean-field dynamo theory. This framework presents much promise for studying the geomagnetic field in a stochastic context.

I. INTRODUCTION

The Earth's magnetic field, also known as the geomagnetic field, is thought to be generated by the movement of conductive, liquid iron in the outer core. Snapshots of the ancient geomagnetic field have been preserved in a variety of different rocks, known in their ensemble as the paleomagnetic record. Paleomagnetic evidence suggests that the geodynamo has been active for at least 3.5 billion years [1, 2]. The geomagnetic field has not remained static throughout its lifetime, varying on a wide range of timescales, from milliseconds to millions of years.

Recent satellite data have enabled detailed studies of the magnetic field's variations on decadal timescales, revealing a rich variety of different waves in the core [3–7]. Studies of the magnetic field's variations on longer timescales are however more challenging, due to a dearth of observations older than a few million years. Furthermore, much of these data do not provide a complete description of the magnetic field, but rather catalogue variations in the dipole component of the field [8–10].

As we do not have a complete description of the geomagnetic field variations over long timescales, it is impossible to create exact models of the geomagnetic field and its history. Nonetheless, the data that we do have may be sufficient to understand the long timescale behaviour of the geodynamo in a statistical manner. Imagine finding an exact copy of planet Earth, or re-starting the Earth's evolution from its formation with the same initial conditions. The processes governing the core flow and magnetic field's evolution are so complex that the chances of the Earth-copy having same magnetic field and velocity structure as the current Earth, at a given age, are essentially zero. Although the system's governing equations are known, an enormous number of parameters can influence its evolution. Let us consider for instance the fluid velocity in the outer core. Amongst other things, the fluid flow will be affected by local variations in temperature, composition and core-mantle boundary topography[11, 12]. Attempting to capture all of these effects exactly is a futile task, similar to trying to model all the forces acting on a Brownian particle (e.g. [13]). More constructively, the geodynamo, like Brownian motion, may be thought of as being stochastic in nature, so that the combined effect of the turbulent and non-linear interactions may be approximated by adding random noise to the velocity term in the governing equations. This transforms the equations into stochastic differential equations (SDEs).

Two complimentary approaches have so far been used to study the stochastic dynamo problem. The first approach [14] assumes that the axial dipole moment (ADM) satisfies a SDE of the form

$$\frac{dX}{dt} = v(X) + g(X)\zeta(t), \tag{1}$$

where X is the ADM, whose time evolution is controlled by two terms. The first, $v(X)$, is known as the drift term, and controls the system's slow, deterministic adjustment towards equilibrium states. The second, $g(X)\zeta(t)$, is the

* dariah@berkeley.edu

noise term, and governs the amplitude of rapid, random fluctuations. Various studies [8, 9, 15, 16] have compiled paleomagnetic observations that may be used to extract statistical properties of the magnetic field, such as the timescale of its correlations or the mean axial dipole moment [14, 17–20]. The drift and noise term in (1) can be directly fit from these observations. This is a useful way of extracting statistical information from the paleomagnetic record, but it means that the physical interpretation of the results is somewhat delicate, as the drift and noise terms are not directly derived from an underlying model of the governing physics. These terms can however be linked to physical models by building stochastic differential equations starting from the governing equations, as done for example in [21, 22]. The stochastic ADM models are thus very useful in bridging the comparisons between the physical stochastic models and the paleomagnetic observations.

This paper takes the second approach, building a physical model for a stochastically forced magnetic field as a starting point from which to compare to paleomagnetic observations. We ask a simple question: what are the magnetic field statistics we expect to observe, assuming that the fluid velocity satisfies certain statistical properties? This question has been considered by many authors, in the field of turbulent fluid dynamics [23–25] and astrophysics [26, 27]. Our aim is to develop a tool specifically tailored to studying the long timescale variations of the Earth's magnetic field. This fundamental problem provides an ideal starting point. We are fortunate that much work has already been done on studying the physics of this problem, as it will allow us to compare our results to existing literature.

For a given velocity field $\mathbf{u}(\mathbf{x}, t)$, the evolution of the magnetic field $\mathbf{B}(\mathbf{x}, t)$ is described by the induction equation

$$\frac{\partial \mathbf{B}}{\partial t} = \nabla \times \left(\mathbf{u} \times \mathbf{B} \right) + \eta \nabla^2 \mathbf{B}, \tag{2}$$

where η is the molecular magnetic diffusivity, thought to be $\eta \sim 0.5 - 1 \ \mathrm{m^2 s^{-1}}$ in Earth's core [28, 29]. Typical values for the root mean squared velocity and magnetic field at the core-mantle boundary are $u_{rms} \sim 0.3 - 0.6 \ \mathrm{mm \ s^{-1}}$ [30] and $\mathrm{B}_{rms} \sim 1 \ \mathrm{mT}$ [31]. In the true physical system, the velocity changes over time, being itself affected by the magnetic field that it generates. The velocity's variations are described by the Navier-Stokes equation, which is coupled to the induction equation through the Lorentz force. This non-linear coupling makes the system of equations challenging to solve. For this reason, we will restrict our attention to the "kinematic dynamo problem", where the velocity is taken to be prescribed and the magnetic field's back reaction is neglected [32]. In contrast to traditional kinematic dynamo studies, we will not specify a particular functional form for the velocity, but rather treat it as a random forcing with well-defined statistical properties.

The problem that we have set out was first considered by Kazantsev [23], who developed a model for magnetic field generation by an isotropically turbulent fluid with infinitesimally short time correlations. This statistical ensemble of velocity fields is commonly known as the "Kraichnan ensemble", as it was independently introduced by Kraichnan in his study of the turbulent advection of passive scalars [33]. Kraichnan also studied the magnetic problem, considering the field excited by a turbulent velocity field that was scale invariant in space and delta correlated in time [24, 25]. This problem has been extended to include further complexities, such as allowing for general velocity time-correlations [34, 35], or compressibility of the fluid [36], which is of great relevance in astrophysical contexts. The system considered in this paper is equivalent to a Kraichnan model with general velocity correlations, studied via functional methods. We are not the first to import mathematical ideas originally used in quantum mechanics to the study of stochastic dynamos. Sokoloff and Yokoi [37] formally solved the induction equation for the magnetic field using a path integral formulation. By assuming a particular form for the velocity correlations and taking the correlation time to be short, they recovered the mean field dynamo equations.

Our aim is to cast this problem in a framework that allows us to study long timescale variations in the geodynamo. Making use of the "Martin-Siggia-Rose-Janssen-De Dominicis" (MSRJD) formalism [38–40], we shall link the velocity's statistical properties (e.g. its correlation function) to those of the magnetic field. Averaging this probability over an ensemble of different realisations of the velocity then allows us to compute information about the expectation value of the magnetic field observables. In essence, the problem will be formulated as an interacting field theory, allowing us to import a vast literature of results and analytical machinery from other disciplines. This has proved successful in the study of a number of related problems, such as in statistical theories of turbulence [41, 42]. Beyond this boon, we hope that by framing the geophysical problem in this manner, we may introduce it to a broader community where these techniques are commonly used.

A problem of particular interest to us, as it has direct applications to data from the paleomagnetic record, is understanding the effect of turbulence on the outer core's magnetic diffusivity. A number of studies [18, 19, 43–45] have shown that, using current estimates for the core's molecular magnetic diffusivity, the time correlations of the magnetic field decay more rapidly than expected for a purely dipolar decay. Davis and Buffett [20] concluded that this rapid decay is not due to a contribution from higher order decay modes, implying that the higher magnetic diffusivity observed in the paleomagnetic record could be attributed to an enhancement of the magnetic diffusivity due to turbulent fluid effects [46]. In this case, the ability to physically link statistical properties of the magnetic

and velocity fields under different assumptions allows us to infer core-properties that are not directly observable, such as the ensemble averaged root-mean squared velocity in the bulk of the outer core. This is particularly significant, since traditional geomagnetic inversion methods only allow us to probe the velocity at the core's surface. The value of developing different approaches to the geodynamo problem lies in establishing new physical connections that allow us to link observables to properties that can only be inferred indirectly. For instance, the field theory framework introduced in this paper can be used to compute arbitrary observables of the magnetic field in terms of the core velocity's statistics. This is extremely useful, as it not only allows us to link the observable part of the magnetic field to the 'hidden' bulk core velocity (which cannot be measured), but provides more detailed information about the core flow's spatial and temporal structure than traditional core flow inversions. These can only describe the flow at the core-mantle boundary, whereas our approach links the magnetic field statistics at the surface of the Earth to average velocities (or derivatives thereof, such as helicity) in the bulk of the core.

Section II begins by setting out the basic problem and the assumptions used to define the velocity's probability distribution. The MSRJD procedure for computing the magnetic field's statistics is outlined in section III. As a first step, we derive an expression for the expectation value of a general magnetic field observable. In section IV we compute the average response (Green) function to first order in the scale of the velocity fluctuations, which enables us to make a new estimate for the effective magnetic diffusivity (section V), taking into account both molecular and turbulent diffusivity contributions. The geophysical implications of our results are discussed in section VI, where we show that our results agree exactly with mean-field theory predictions. A demonstration of how the response and diffusivity calculations can be extended to higher order in the velocity in the limit of small correlation times is outlined in section VII. Our conclusions are finally presented in section VIII.

II. PROBLEM SET-UP

We wish to study the statistics of a magnetic field $\mathbf{B}(\mathbf{x}, t)$, under the influence of isotropic turbulence. The evolution of the magnetic field is governed by the induction equation (2), subject to the usual requirement that

$$\nabla \cdot \mathbf{B} = 0. \tag{3}$$

Turbulent effects enter the equation through the velocity, $\mathbf{u}(\mathbf{x}, t)$, which is not prescribed to a single functional form, but rather acts as a random forcing with well-defined Gaussian statistics. The velocity's probability distribution is taken to be

$$p[\mathbf{u}] = N \exp\left[-\frac{1}{2} \int d\mathbf{x} \, d\mathbf{x}' \, dt \, dt' \, u_j(\mathbf{x}, t) C_{jk}^{-1}(\mathbf{x} - \mathbf{x}', t - t') u_k(\mathbf{x}', t') \right], \tag{4}$$

where N is the normalisation. This distribution has vanishing mean

$$\langle \mathbf{u}(\mathbf{x}, t) \rangle_u = \mathbf{0}, \tag{5}$$

and correlations

$$\langle u_j(\mathbf{x}, t) u_k(\mathbf{x}', t') \rangle_u = C_{jk}(\mathbf{x} - \mathbf{x}', t - t'). \tag{6}$$

The angle brackets $\langle \ldots \rangle_u$ denote averaging over all possible realisations of the velocity field. The velocity's correlation function in space and time is $C_{jk}(\mathbf{x} - \mathbf{x}', t - t')$. Note that we have chosen the correlation to have both space and time translation invariance, so that we are considering an isotropic medium. The incompressibility condition $\nabla \cdot \mathbf{u} = 0$ is imposed by requiring $\partial_j C_{jk} = \partial_k C_{jk} = 0$. It is of course possible to include a mean fluid flow, though we shall restrict our attention to the zero-mean case. The correlation function for the fluid velocity in the Earth's core is unknown, as are its correlation length and time. These parameters may however be estimated through scaling arguments and extrapolations from geodynamo simulations [13, 46], and appear to be on the order $\ell \sim 10^5$ m and $\tau \sim 10^2$ years, which is short compared to convective overturn times of ~ 150 years.

Throughout this paper, the convention will be to denote the arguments of functions using parentheses (e.g. $f(\mathbf{x})$), while the arguments of functionals will be denoted with square brackets, as in $F[f(\mathbf{x})]$. In this study we do not consider the spherical geometry relevant to planetary bodies, but rather assume that fields are distributed over all space. The next section outlines the MSRJD procedure for computing magnetic field observables given these velocity statistics.

III.   MSRJD PROCEDURE

For brevity, we will only sketch out the main ideas behind the MSRJD procedure in this section. A step-by-step explanation of this procedure is provided in Appendix A.

Our aim is to compute observables of the magnetic field given that we know its evolution equation and the statistics of $\mathbf{u}$, subject to (3). This constraint may be enforced by expressing the magnetic field in terms of the magnetic vector potential $\mathbf{A}(\mathbf{x}, t)$, such that $\mathbf{B} = \nabla \times \mathbf{A}$. Complete information of the magnetic vector potential's statistics will allow us to compute any magnetic field statistics. Written in terms of $\mathbf{A}$, the induction equation (2) becomes

$$\frac{\partial \mathbf{A}}{\partial t} = \mathbf{u} \times (\nabla \times \mathbf{A}) + \eta \nabla^2 \mathbf{A} + \nabla \chi, \tag{7}$$

where χ is an arbitrary scalar. The freedom to choose the potential $\nabla \chi$ is equivalent to the freedom to choose $\mathbf{A}$'s gauge. This allows us to simply set $\chi = 0$, effectively absorbing it into the gauge function φ. We must then remember that $\mathbf{A}$ is invariant under all gauge transformations $\mathbf{A} \to \mathbf{A} + \nabla \varphi$. This invariance requires careful treatment in the MSRJD procedure, addressed in Appendix C. Equation (7) may be written schematically as

$$(\mathcal{L}_0 + \mathcal{L}(\mathbf{u})) \, \mathbf{A} = \mathbf{0}, \tag{8}$$

where the operators $\mathcal{L}_0$ and $\mathcal{L}(\mathbf{u})$ encode the diffusive behaviour and interaction with the velocity respectively. The expectation value of an observable $\langle O[\mathbf{A}] \rangle$, in general a functional of $\mathbf{A}$, is given by

$$\langle O[\mathbf{A}] \rangle = \int \mathcal{D}\mathbf{A} \mathcal{D}\mathbf{u} \; p[\mathbf{A}, \mathbf{u}] O[\mathbf{A}]. \tag{9}$$

Evaluating this average requires knowledge of the joint probability of finding a particular $\mathbf{A}$ and $\mathbf{u}$ at all points in space and time, $p[\mathbf{A}, \mathbf{u}]$, which is made possible by using functional methods borrowed from field theory. The integrals $\int \mathcal{D}\mathbf{A}$ and $\int \mathcal{D}\mathbf{u}$ denote functional (path) integrals over all possible $\mathbf{A}(\mathbf{x}, t)$ and $\mathbf{u}(\mathbf{x}, t)$ respectively. Given that we have an assumed probability distribution for the velocity, we would like to separate the joint probability into an expression that includes $p[\mathbf{u}]$, so that all possible velocity realisations may be integrated over. The joint probability may be expressed as

$$p[\mathbf{A}, \mathbf{u}] = p[\mathbf{A}|\mathbf{u}] p[\mathbf{u}], \tag{10}$$

where $p[\mathbf{A}|\mathbf{u}]$ is the conditional functional probability distribution of $\mathbf{A}$ given $\mathbf{u}$. This probability requires $\mathbf{A}$ to both solve the induction equation (2) and satisfy the appropriate boundary conditions at each point in space and time for any given $\mathbf{u}$. Denoting the $\mathbf{A}$ that solves (7) as $\mathbf{A}^*$, we may write the probability of observing $\mathbf{A}$ for a given realisation of $\mathbf{u}$ as

$$p[\mathbf{A}|\mathbf{u}] = \delta\big[\mathbf{A} - \mathbf{A}^*(\mathbf{u})\big]. \tag{11}$$

Following the procedure outlined in Appendix A, we may transform the argument of the delta function in (11) to be of the form $\delta[(\mathcal{L}_0 + \mathcal{L}(\mathbf{u})) \, \mathbf{A}]$. This delta function constraint is imposed by writing it as its Fourier transform, which introduces the auxiliary function $\tilde{\mathbf{A}}$. The average in (9) is then

$$\langle O[\mathbf{A}] \rangle = \mathcal{N} \int \mathcal{D}\mathbf{A} \mathcal{D}\tilde{\mathbf{A}} \; O[\mathbf{A}] \exp\left[i \int \tilde{\mathbf{A}} \mathcal{L}_0 \mathbf{A} \right] \int \mathcal{D}\mathbf{u} \, p[\mathbf{u}] \exp\left[i \int \tilde{\mathbf{A}} \mathcal{L}(\mathbf{u}) \mathbf{A} \right], \tag{12}$$

where $\mathcal{N}$ is the normalisation constant and the fields' and integrals' arguments have been kept implicit for notational clarity. Since $\mathcal{L}(\mathbf{u})$ is linear in $\mathbf{u}$ and $p[\mathbf{u}]$ is Gaussian, the probability distribution's average over all possible realisations of the velocity is given by a Gaussian integral, such that (12) becomes

$$\langle O[\mathbf{A}] \rangle = \mathcal{N} \int \mathcal{D}\mathbf{A} \mathcal{D}\tilde{\mathbf{A}} \; O[\mathbf{A}] \exp\left[-S_0[\mathbf{A}, \tilde{\mathbf{A}}] - S_{\text{int}}[\mathbf{A}, \tilde{\mathbf{A}}, \mathbf{C}] \right]. \tag{13}$$

Equation (13) introduces the *action* $S[\mathbf{A}, \tilde{\mathbf{A}}] = S_0[\mathbf{A}, \tilde{\mathbf{A}}] + S_{\text{int}}[\mathbf{A}, \tilde{\mathbf{A}}, \mathbf{C}]$, where $S_0[\mathbf{A}, \tilde{\mathbf{A}}]$ (the "free action") is the contribution we would have from free decay (i.e. $\mathbf{u} = \mathbf{0}$), while $S_{\text{int}}[\mathbf{A}, \tilde{\mathbf{A}}, \mathbf{C}]$ (the "interaction action") represents the interaction between the magnetic field and the velocity, and depends on the velocity's correlations $\mathbf{C}$. These are respectively

$$
\begin{aligned}
S_0 &= -i \int d\mathbf{x} \; dt \; \tilde{\mathbf{A}} \cdot \left(\partial_t \mathbf{A} - \eta \nabla^2 \mathbf{A} \right) = -i \int d\mathbf{x} \; d\mathbf{x}' \; dt \; dt' \; \tilde{\mathbf{A}}(\mathbf{x}', t') \cdot g_0^{-1}(\mathbf{x}, \mathbf{x}', t, t') \cdot \mathbf{A}(\mathbf{x}, t), \text{ and} \\
S_{\text{int}} &= \frac{1}{2} \int d\mathbf{x} \; d\mathbf{x}' \; dt \; dt' \left[\varepsilon_{jab} (\nabla \times \mathbf{A})_a(\mathbf{x}, t) \tilde{A}_b(\mathbf{x}, t) C_{jk}(\mathbf{x}, \mathbf{x}', t, t') \varepsilon_{kcd} (\nabla \times \mathbf{A})_c(\mathbf{x}', t') \tilde{A}_d(\mathbf{x}', t') \right].
\end{aligned}
\tag{14}
$$

The summation convention is used here and throughout the paper. Note that the purely diffusive operator $\partial_t - \eta\nabla^2$ is written as the inverse of its Green function, g_0. Comparing (13) to

$$\langle O[\mathbf{A}]\rangle = \int \mathcal{D}\mathbf{A}\mathcal{D}\tilde{\mathbf{A}} \; O[\mathbf{A}]p[\mathbf{A}, \tilde{\mathbf{A}}], \tag{15}$$

we see that the newly defined probability distribution for $\mathbf{A}$ and $\tilde{\mathbf{A}}$ is

$$p[\mathbf{A}, \tilde{\mathbf{A}}] = \mathcal{N}\exp\big[- S_0[\mathbf{A}, \tilde{\mathbf{A}}] - S_{\text{int}}[\mathbf{A}, \tilde{\mathbf{A}}, \mathbf{C}]\big]. \tag{16}$$

This quantity will allow us to compute observables of $\mathbf{A}$ that can be directly related to observables of the magnetic field. For our purposes, it is more convenient to Fourier transform (14) in both space and time. In Fourier space, the velocity's correlations may be written as

$$\langle u_j(\mathbf{q}, \omega)u_k(\mathbf{q}', \omega')\rangle = (2\pi)^4\delta(\mathbf{q} + \mathbf{q}')\delta(\omega + \omega')C_{jk}(\mathbf{q}, \omega), \tag{17}$$

where $\mathbf{q}$ and $\mathbf{q}'$ are wavevectors. Due to incompressibility, imposed by $q_jC_{jk} = q_kC_{jk} = 0$, the correlations are restricted to the form [32]

$$C_{jk}(\mathbf{q}, \omega) = \gamma(\mathbf{q}, \omega)\sigma_{jk}(\mathbf{q}) + i\alpha(\mathbf{q}, \omega)\varepsilon_{ijk}q_i \qquad \text{where} \qquad \sigma_{jk}(\mathbf{q}) = \delta_{jk} - \frac{1}{q^2}q_jq_k. \tag{18}$$

In this paper, we wish to consider the case of isotropic turbulence. Isotropy requires C_{jk} to be a symmetric tensor, so that the $i\alpha(\mathbf{q}, \omega)\varepsilon_{ijk}q_i$ term vanishes. This anti-symmetric term is responsible for generating an alpha effect, whereby localised helical fluid disturbances twist the magnetic field lines in such a way as to generate new current parallel to the original field. The alpha term represents an effective electromotive force on the magnetic field (sometimes referred to as a 'mass term' in field theory). This term can be easily reintroduced into C_{jk} without altering the formalism; it would simply make the expressions more complex. Following the procedure outlined in Appendix B, in essence an application of the convolution theorem, the Fourier transform of the interaction action may be written

$$S_{\text{int}} = -\frac{1}{2}\int d\mkern-9mu/\,\mathbf{p}\,d\mkern-9mu/\,\mathbf{p}'d\mkern-9mu/\,\mathbf{q}\,d\mkern-9mu/\,\omega\,d\mkern-9mu/\,\omega'd\mkern-9mu/\,\Omega \; A_\alpha(\mathbf{p}, \omega)\tilde{A}_\beta(-\mathbf{p} - \mathbf{q}, -\omega - \Omega)M^{kl}_{\alpha\beta\gamma\delta}(\mathbf{q}, \Omega)p_kp'_lA_\gamma(\mathbf{p}', \omega')\tilde{A}_\delta(\mathbf{q} - \mathbf{p}', \Omega - \omega')$$

$$\text{with} \quad M^{kl}_{\alpha\beta\gamma\delta}(\mathbf{q}, \Omega) = \big(\delta_{k\beta}\delta_{l\delta}\sigma_{\alpha\gamma}(\mathbf{q}) - \delta_{\alpha\beta}\delta_{l\delta}\sigma_{k\gamma}(\mathbf{q}) - \delta_{k\beta}\delta_{\gamma\delta}\sigma_{\alpha l}(\mathbf{q}) + \delta_{\alpha\beta}\delta_{\gamma\delta}\sigma_{kl}(\mathbf{q})\big)\gamma(\mathbf{q}, \Omega), \tag{19}$$

where $\mathbf{p}$, $\mathbf{p}'$ and $\mathbf{q}$ are newly defined wavevectors, ω, ω' and Ω are conjugate frequencies, and the bar on the integration measure represents a division by 2π for each dimension, i.e. $d\mkern-9mu/\,\mathbf{p} = \dfrac{d\mathbf{p}}{(2\pi)^3}$ and $d\mkern-9mu/\,\omega = \dfrac{d\omega}{2\pi}$. The Fourier transform of the free action is

$$S_0 = -i\int d\mkern-9mu/\,\mathbf{q}\;d\mkern-9mu/\,\omega\;\big(i\omega + \eta q^2\big)\,\tilde{\mathbf{A}}(-\mathbf{q}, -\omega)\cdot\mathbf{A}(\mathbf{q}, \omega). \tag{20}$$

IV. AVERAGE FIRST ORDER RESPONSE

The MSRJD procedure gives us a means of calculating observables of the magnetic field. We may now compute the expected turbulent diffusivity η_t by finding an average Green (response) function for our system and considering the coefficient of the diffusive term. Our results may be compared directly to the work of Moffatt [32] and Kazantsev [23], allowing us to benchmark our method against known results.

A. Response function formalism

We make use of the response function formalism [47] to calculate the magnetic field's Green function. Consider adding a small arbitrary forcing $\mathbf{h}$ to the equation for the magnetic vector potential (7), so that

$$\frac{\partial\mathbf{A}}{\partial t} = \mathbf{u}\times(\nabla\times\mathbf{A}) + \eta\nabla^2\mathbf{A} + \mathbf{h}. \tag{21}$$

Solutions to this equation may be written as

$$A_\alpha(\mathbf{x}, t) = \int d\mathbf{x}'dt'G_{\alpha\beta}(\mathbf{x}, \mathbf{x}', t, t')h_\beta(\mathbf{x}', t'), \tag{22}$$

where $G_{\alpha\beta}(\mathbf{x}, \mathbf{x}', t, t')$ is the Green function for the induction equation in physical space in the absence of the forcing $\mathbf{h}$. In Fourier space, (22) becomes

$$A_\alpha(\mathbf{k}, \omega) = \int d\mathbf{k}_2 \, d\omega_2 G_{\alpha\beta}(\mathbf{k}, \mathbf{k}_2, \omega, \omega_2) h_\beta(-\mathbf{k}_2, -\omega_2). \tag{23}$$

The forcing $\mathbf{h}(\mathbf{k}, \omega)$ is independent of both $\mathbf{u}$ and $\mathbf{A}$, so averaging does not affect it. Taking the functional derivative of the ensemble average of (23) with respect to $h_\beta(-\mathbf{k}', -\omega')$, we find

$$\left. \frac{\delta\langle A_\alpha(\mathbf{k}, \omega)\rangle}{\delta h_\beta(-\mathbf{k}', -\omega')} \right|_{\mathbf{h}=0} = \int d\mathbf{k}_2 d\omega_2 \, \langle G_{\alpha\beta}(\mathbf{k}, \mathbf{k}_2, \omega, \omega_2)\rangle \, \delta(\mathbf{k}_2 - \mathbf{k}') \delta(\omega_2 - \omega') = (2\pi)^{-4} \langle G_{\alpha\beta}(\mathbf{k}, \mathbf{k}', \omega, \omega')\rangle. \tag{24}$$

The LHS of this expression defines the average Green function $\langle G_{\alpha\beta}(\mathbf{k}, \mathbf{k}', \omega, \omega')\rangle$. To evaluate it, we require an expression for $\langle A_\alpha(\mathbf{k}, \omega)\rangle$. Repeating the steps prescribed by the MSRJD procedure, we find an expression analogous to (13), but with an additional $\mathbf{h}$-dependent factor in the exponent

$$\langle O[\mathbf{A}]\rangle = \mathcal{N} \int \mathcal{D}\mathbf{A}\mathcal{D}\tilde{\mathbf{A}} \, O[\mathbf{A}] \exp\left[- S_0[\mathbf{A}, \tilde{\mathbf{A}}] - S_{\text{int}}[\mathbf{A}, \tilde{\mathbf{A}}, \mathbf{C}] - i \int d\mathbf{k} d\omega \, \tilde{\mathbf{A}}(\mathbf{k}, \omega) \cdot \mathbf{h}(-\mathbf{k}, -\omega) \right]. \tag{25}$$

Using (24) and (25), the average Green function is found to be

$$\langle G_{\alpha\beta}(\mathbf{k}, \mathbf{k}', \omega, \omega')\rangle = -i\langle \mathbf{A}_\alpha(\mathbf{k}, \omega)\tilde{\mathbf{A}}_\beta(\mathbf{k}', \omega')\rangle. \tag{26}$$

This is a very useful relation, as it allows us to compute the average Green function for the vector potential directly from the correlations of $\mathbf{A}$ and $\tilde{\mathbf{A}}$. We may then obtain the magnetic field's response by relating it to $G(\mathbf{k}, \mathbf{k}', \omega, \omega')$.

Denote the Green function for the induction equation (2) as $\mathcal{G}(\mathbf{k}, \mathbf{k}', \omega, \omega')$. The fictitious force $\mathbf{h}$ in (21) becomes $i\mathbf{k} \times \mathbf{h}(\mathbf{k}, \omega)$ in the induction equation, therefore magnetic field solutions are written

$$\langle B_\alpha(\mathbf{k}, \omega)\rangle = -i \int d\mathbf{k}_2 \, d\omega_2 \langle \mathcal{G}_{\alpha b}(\mathbf{k}, \mathbf{k}_2, \omega, \omega_2)\rangle \varepsilon_{bij}(k_2)_i h_j(-\mathbf{k}_2, -\omega_2). \tag{27}$$

Taking the functional derivative with respect to $h_\psi(-\mathbf{k}', -\omega')$, we obtain

$$\frac{\delta\langle B_\alpha(\mathbf{k}, \omega)\rangle}{\delta h_\psi(-\mathbf{k}', -\omega')} = -i\langle \mathcal{G}_{\alpha b}(\mathbf{k}, \mathbf{k}', \omega, \omega')\rangle \varepsilon_{bi\psi} k_i'. \tag{28}$$

To isolate $\langle \mathcal{G}_{\alpha b}(\mathbf{k}, \mathbf{k}', \omega, \omega')\rangle$, we operate $\mathbf{k}' \times = \varepsilon_{\beta n\psi} k_n'$ on (28), and find

$$\langle \mathcal{G}_{\alpha\beta}(\mathbf{k}, \mathbf{k}', \omega, \omega')\rangle = \frac{i}{(k')^2}\varepsilon_{\beta n\psi} k_n' \frac{\delta\langle B_\alpha(\mathbf{k}, \omega)\rangle}{\delta h_\psi(-\mathbf{k}', -\omega')}. \tag{29}$$

Note that we have used the relation $\mathbf{k} \cdot \mathcal{G}(\mathbf{k}, \mathbf{k}', \omega, \omega') = 0$, which must hold to enforce the condition $\nabla \cdot \mathbf{B} = 0$. The magnetic field is related to the vector potential by

$$B_\alpha(\mathbf{k}, \omega) = i\varepsilon_{\alpha l\phi} k_l A_\phi(\mathbf{k}, \omega), \tag{30}$$

so

$$\mathcal{G}_{\alpha\beta}(\mathbf{k}, \mathbf{k}', \omega, \omega') = -\frac{1}{(k')^2}\varepsilon_{\alpha l\phi}\varepsilon_{\beta n\psi} k_n' k_l G_{\phi\psi}(\mathbf{k}, \mathbf{k}', \omega, \omega'). \tag{31}$$

Through (31) we have a relation between $G(\mathbf{k}, \mathbf{k}', \omega, \omega')$ and $\mathcal{G}(\mathbf{k}, \mathbf{k}', \omega, \omega')$. Let us now consider what these functions are when the interaction term is included to first order.

B. Diagrams for computing interaction correlations

Computing $\mathcal{G}(\mathbf{k}, \mathbf{k}', \omega, \omega')$ involves finding the correlation of the vector potential with its conjugate field, as can be seen from eqs. (26) and (31). To first order, we may write

$$\langle A_\psi(\mathbf{k}, \omega)\tilde{A}_\phi(\mathbf{k}', \omega')\rangle = \mathcal{N} \int \mathcal{D}\mathbf{A}\mathcal{D}\tilde{\mathbf{A}} \, A_\psi(\mathbf{k}, \omega)\tilde{A}_\phi(\mathbf{k}', \omega')e^{-S_0[\mathbf{A}, \tilde{\mathbf{A}}]} \left[1 - S_{\text{int}}[\mathbf{A}, \tilde{\mathbf{A}}, \mathbf{C}] \right] + O(S_{\text{int}}^2), \tag{32}$$

$$\underset{(\mathbf{k},\omega,\psi)}{\text{O}\!\!-\!\!-\!\!-\!\!-\!\!-}\underset{(\mathbf{k}',\omega',\phi)}{-\!\!-\!\!-\!\!-\!\!-\text{O}} = i\delta_{\psi\phi}(2\pi)^4\delta(\mathbf{k}+\mathbf{k}')\delta(\omega+\omega')g_0(\mathbf{k},\omega)$$

FIG. 1. This diagram represents the zero order propagator, $\langle A_\psi(\mathbf{k},\omega)\tilde{A}_\phi(\mathbf{k}',\omega')\rangle_0$. $\mathbf{A}$ is denoted by the solid line, while $\tilde{\mathbf{A}}$ is denoted by the dashed line. The wavevector, frequency and index of each is given below the lines in brackets. $g_0(\mathbf{k},\omega)$ is defined in (35).
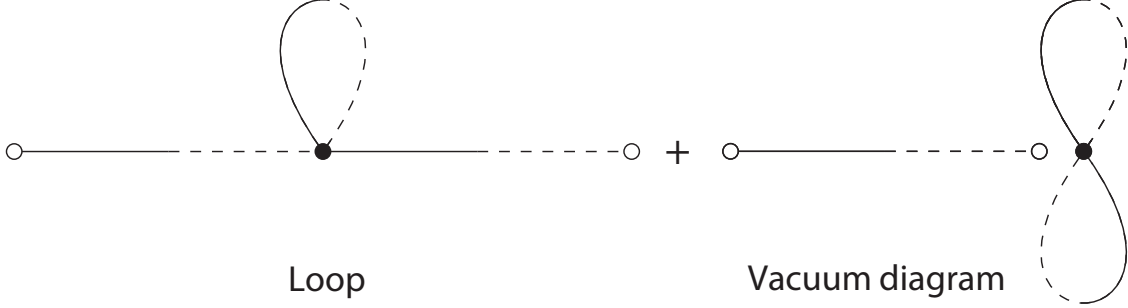

Loop   Vacuum diagram

FIG. 2. First order contributions to the average $\langle A_\psi(\mathbf{k},\omega)\tilde{A}_\phi(\mathbf{k}',\omega')\rangle$. Only the loop diagrams (left) contribute to this average.

where the interaction action is given by (19). By taking the expansion to first order, we are assuming that the magnitude of the velocity correlation function $\gamma(\mathbf{q},\omega)$ is small. Computing (32) to first order requires the average

$$\langle A_\psi(\mathbf{k},\omega)\tilde{A}_\phi(\mathbf{k}',\omega')A_\alpha(\mathbf{p},\omega_1)\tilde{A}_\beta(-\mathbf{p}-\mathbf{q},-\omega_1-\Omega)A_\gamma(\mathbf{p}',\omega_2)\tilde{A}_\delta(\mathbf{q}-\mathbf{p}',\Omega-\omega_2)\rangle. \tag{33}$$

As this average is Gaussian, we may employ Wick's theorem [48] to rewrite it in terms of a sum of all possible pairwise contractions of the form $\langle\tilde{A}_i(\mathbf{k},\omega)A_j(\mathbf{k}',\omega')\rangle$. There are $^6C_2 = 15$ different combinations, some of which will vanish. The easiest way to write down these different combinations and determine all non-zero contributions is by using a diagrammatic approach pioneered by Feynman [49]. Each Feynman diagram represents an integral contributing to the average (32).

It is helpful to introduce some commonly used naming conventions [50]. The diagrams' lines can be separated into two types, *external* and *internal*. External lines have a free end (indicated by an empty circle) that is not connected to anything, and specify the quantities to be measured. Vertices are the points where two or more lines join together. Internal lines are those joining two vertices together. Diagrams without external lines are known as vacuum diagrams.

Having laid out the basic terminology, we must establish a convention for our specific case. The rules for the diagrams describing our system are summarised below.

- $A_\psi(\mathbf{k},\omega)$ is represented by a solid line, while $\tilde{A}_\phi(\mathbf{k}',\omega')$ is represented by a dashed line. Each line is labelled by its argument and the vector's index, in the form (*arg, index*).

- Connected lines contribute a factor of

$$(2\pi)^4\delta(\mathbf{k}+\mathbf{k}')\delta(\omega+\omega')\ g_0(\mathbf{k},\omega), \tag{34}$$

  with all $\mathbf{k}$ and ω from internal lines integrated over, where

$$g_0(\mathbf{k},\omega) = (i\omega+\eta k^2)^{-1}. \tag{35}$$

- Given that the auto-correlations of $\mathbf{A}$ vanish (see (C.9)), the only connections that ensure a non-zero contribution are those between a solid and dashed line.

- Vertices are denoted by a filled circle. They contribute a factor of $M^{kl}_{\alpha\beta\gamma\delta}(\mathbf{q},\Omega)p_kp'_l$ to the integral, and must be connected to four lines representing $A_\alpha(\mathbf{p},\omega_1)$, $\tilde{A}_\beta(-\mathbf{p}-\mathbf{q},-\omega_1-\Omega)$, $A_\gamma(\mathbf{p}',\omega_2)$ and $\tilde{A}_\delta(\mathbf{q}-\mathbf{p}',\Omega-\omega_2)$. The number of vertices gives the order to which $\gamma(\mathbf{q},\omega)$ appears.

The zero-order contribution to the average (32) is drawn diagrammatically in Figure 1. The beginning and end of the diagram are denoted by two circles, connected to lines representing $A_\psi(\mathbf{k},\omega)$ and $\tilde{A}_\phi(\mathbf{k}',\omega')$ respectively. The

connection between the two lines represents the average $\langle A_\psi(\mathbf{k}, \omega) \tilde{A}_\phi(\mathbf{k}', \omega') \rangle_0$. Compared to the zero-order diagram, the first order diagrams gain an interaction vertex. All possible types of first order diagram are shown in Fig. 2. Note that vacuum diagrams (where the loops are separated from the external lines) do not contribute, as they are cancelled by the normalisation. This is referred to as the "linked cluster theorem" [48]. Extensions to higher order involve two or more loops and interaction vertices. Since any combinations involving two $\mathbf{A}$s vanish, we need only consider diagrams where $\mathbf{A}$ and $\tilde{\mathbf{A}}$ connect. We are left with four unique non-zero combinations, labelled $I_\alpha, I_\beta, I_\gamma$ and I_δ, illustrated in Fig. 3. For the sake of brevity, we relegate the calculations to Appendix D, and list the contributions to (32) below. The I_α and I_δ contributions are, respectively,

$$-\frac{i}{2}G_0^2(\mathbf{k}, \omega)\delta(\mathbf{k}+\mathbf{k}')\delta(\omega+\omega')\int d\mathbf{q}d\Omega \; \gamma(\mathbf{q}, \Omega)g_0(\mathbf{k}-\mathbf{q}, \omega-\Omega)\left[\delta_{\psi\phi}\left(k^2 - \frac{(\mathbf{k}\cdot\mathbf{q})^2}{q^2}\right) - k_k(\mathbf{k}-\mathbf{q})_l\delta_{k\psi}\sigma_{\phi l}\right], \quad (36)$$

$$-\frac{i}{2}G_0^2(\mathbf{k}, \omega)\delta(\mathbf{k}+\mathbf{k}')\delta(\omega+\omega')\int d\mathbf{q}d\Omega \; \gamma(\mathbf{q}, \Omega)g_0(\mathbf{k}+\mathbf{q}, \omega+\Omega)\left[\delta_{\psi\phi}\left(k^2 - \frac{(\mathbf{k}\cdot\mathbf{q})^2}{q^2}\right) - k_k(\mathbf{k}+\mathbf{q})_l\delta_{k\psi}\sigma_{\phi l}\right]. \quad (37)$$

Note that the only difference between I_α and I_δ is the sign between the arguments of the g_0 under the integral. It transpires that the I_β and I_γ diagrams cannot contribute to the magnetic field's Green function due to their index structure (see Appendix D). Overall, the relevant interaction contribution to the vector potential's Green function is

$$G_{\psi\phi}^{int}(\mathbf{k}, \mathbf{k}', \omega, \omega') = -i(I_\alpha + I_\delta). \quad (38)$$

Making use of (31), (36) and (37), we finally find the magnetic field's Green function to first order to be

$$\mathcal{G}_{\alpha\beta}(\mathbf{k}, \mathbf{k}', \omega, \omega') = (2\pi)^4\delta(\mathbf{k}+\mathbf{k}')\delta(\omega+\omega')\sigma_{\alpha\beta}(\mathbf{k})g(k, \omega), \quad (39)$$

where $g(k, \omega)$ is defined as

$$g(k, \omega) = \frac{1}{i\omega + \eta k^2}\left[1 - \frac{1}{2}\int d\mathbf{q}d\Omega\frac{k^2 - q^{-2}(\mathbf{q}\cdot\mathbf{k})^2}{i\omega + \eta k^2}\left(\frac{\gamma(\mathbf{q}, \Omega)}{i(\omega-\Omega) + \eta(\mathbf{k}-\mathbf{q})^2} + \frac{\gamma(\mathbf{q}, \Omega)}{i(\omega+\Omega) + \eta(\mathbf{k}+\mathbf{q})^2}\right)\right]. \quad (40)$$

Having found $\mathcal{G}$, we may now ask how the fluid flow's turbulent behaviour affects physical properties of the system, such as the magnetic diffusivity.

V. TURBULENT DIFFUSIVITY

Let us begin by considering how the diffusivity is defined. Generally, it may be thought of as the coefficient of the induction equation's Laplacian term in physical space, or the k^2 term in Fourier space. In the zero-order case, the Green function is

$$\mathcal{G}_{\alpha\beta}^0(\mathbf{k}, \mathbf{k}', \omega, \omega') = (2\pi)^4\delta(\mathbf{k}+\mathbf{k}')\delta(\omega+\omega')\sigma_{\alpha\beta}(\mathbf{k})g_0(k, \omega). \quad (41)$$

The delta functions reflect the spatial and temporal translation invariance, while $\sigma_{\alpha\beta}(\mathbf{k})$ guarantees the magnetic field's solenoidality. All system-specific information is contained in $g_0(k, \omega)$. Denoting the solution to $g_0^{-1}(\omega_0^*, k) = 0$ as $\omega_0^*(k)$, we may write $\omega_0^* = i\eta k^2$. These solutions are the poles of $g_0(k, \omega)$ and the reciprocals of the decay times. From the definition of ω_0^*, we see that

$$\eta = \frac{1}{2i}\frac{\partial^2\omega_0^*}{\partial k^2}\bigg|_{k=0} \quad (42)$$

is a valid definition for the diffusion coefficient. We may use this expression to compute a new effective magnetic diffusivity, by taking into account the interaction between the magnetic field and the velocity. Let us write the Green function as

$$g(k, \omega) = i\omega + \eta_{\text{eff}}k^2 + \ldots, \quad (43)$$

where η_{eff} is a modified diffusivity and '...' represents more complex terms that might contribute to the response. To find an expression for η_{eff}, we require the inverse of (39). Note that $g(k, \omega)$, defined in (40), may be written in terms of $g_0(k, \omega)$ as

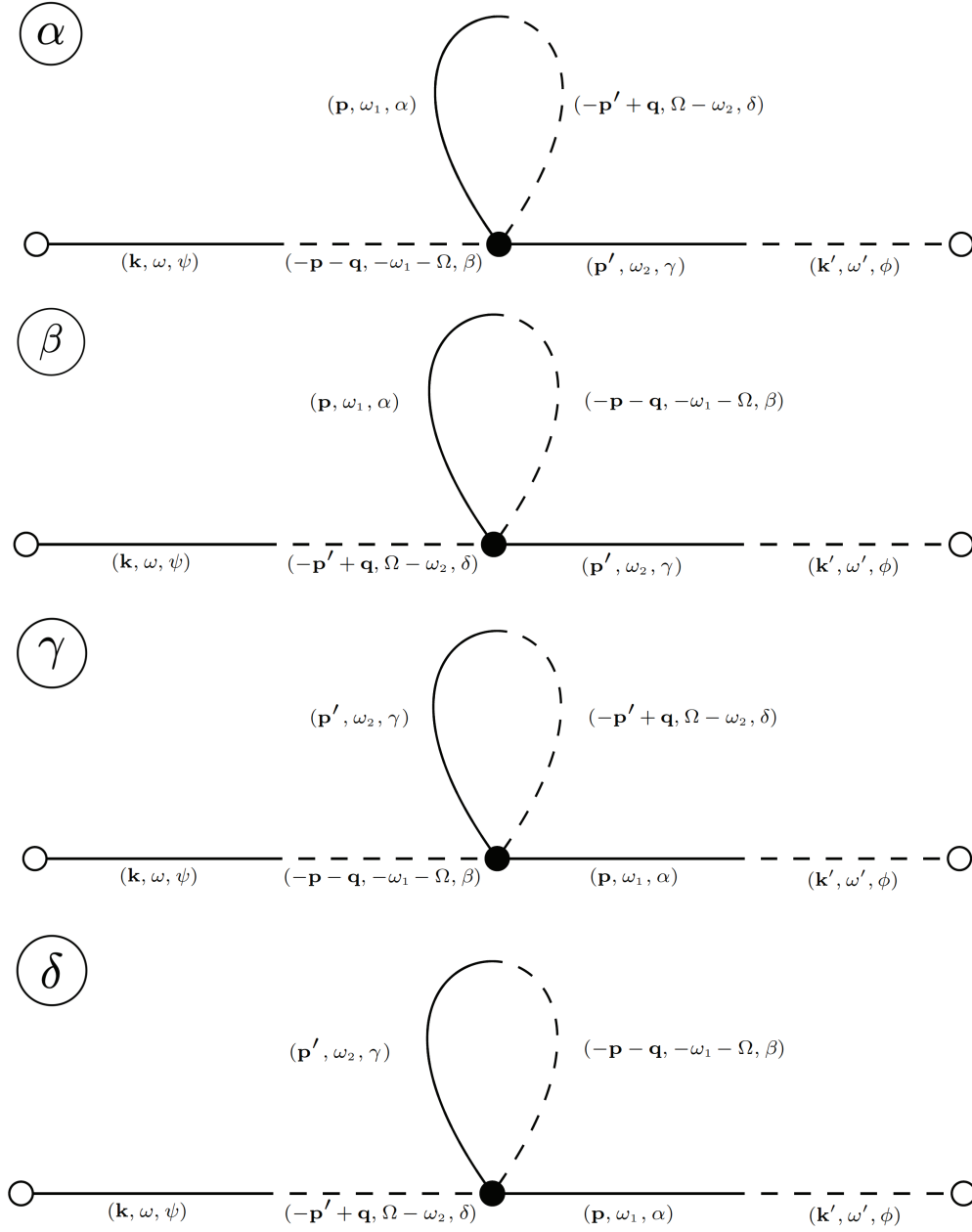$$g(k, \omega) = g_0(k, \omega)\left[1 - g_0(k, \omega)k^2F(k, \omega)\right], \quad (44)$$

FIG. 3. The non-zero first order diagrams whose sum represents the quantity (33) after applying Wick's theorem. The notation is the same as in Fig. 1. The vertices (black dots) contribute a factor of $M^{kl}_{\alpha\beta\gamma\delta}(\mathbf{q}, \Omega)p_k p'_l$.

where

$$F(k,\omega) = \frac{1}{2} \int d\!\!\!{}^-\mathbf{q}\, d\!\!\!{}^-\Omega \left(1 - \cos^2\theta\right) \left[\frac{\gamma(\mathbf{q}, \Omega)}{i(\omega - \Omega) + \eta(\mathbf{k} - \mathbf{q})^2} + \frac{\gamma(\mathbf{q}, \Omega)}{i(\omega + \Omega) + \eta(\mathbf{k} + \mathbf{q})^2} \right], \tag{45}$$

and the angle between $\mathbf{k}$ and $\mathbf{q}$ has been labelled θ. Assuming that the first order correction is small, we have

$$g^{-1}(k,\omega) \approx g_0^{-1}(k,\omega) + k^2 F(k,\omega). \tag{46}$$

Let us now look for the poles of $g(k,\omega)$ by solving $g^{-1}(\omega^*, k) = 0$ for $\omega^*(k)$. From (46) we see that they must occur when

$$\omega^*(k) = i\eta k^2 + ik^2 F(k, \omega^*). \tag{47}$$

Following (42), we may find the new effective diffusivity by considering

$$\eta_{\text{eff}} = \frac{1}{2i} \frac{\partial^2 \omega^*}{\partial k^2}\bigg|_{k=0} = \eta + F(0, \omega^*(0)). \tag{48}$$

The first term is of course the zero-order molecular diffusivity, while the second term constitutes the contribution from the turbulent diffusivity, η_t. Given that $\omega^*(0) = 0$,

$$\eta_t = \int d\mathbf{q} d\Omega \; \gamma(\mathbf{q}, \Omega) \left(1 - \cos^2 \theta\right) \frac{\eta q^2}{\Omega^2 + \eta^2 q^4}. \tag{49}$$

Expression (49) gives us a quantitative estimate of the turbulent magnetic diffusivity in terms of the velocity's correlation function. The form of (49) provides insight into the origin of η_t. The turbulent diffusivity vanishes when $\theta = 0$ ($\mathbf{k} \parallel \mathbf{q}$) and is maximal when $\theta = \pi/2$ ($\mathbf{k} \perp \mathbf{q}$). For plane wave velocity and magnetic field disturbances, $\mathbf{q}$ and $\mathbf{k}$ may be interpreted as wavevectors perpendicular to the respective disturbances' wavefronts. When the wavevectors $\mathbf{k}$ and $\mathbf{q}$ are parallel, the velocity and magnetic field must be co-planar, since they are both divergenceless. The inductive term in (2) must therefore vanish, as the cross product is parallel to $\mathbf{k}$ (or $\mathbf{q}$). This picture is consistent with the notion of the fluid velocity lifting the magnetic field out of its plane, and in doing so creating new current loops that interact with the existing field. The strength of the velocity correlations is encapsulated in $\gamma(\mathbf{q}, \Omega)$; stronger fluctuations lead directly to larger η_t.

Assuming that $\gamma(\mathbf{q}, \Omega)$ only depends on the magnitude $|\mathbf{q}| = q$ (isotropic approximation), we may integrate over the solid angle, and find

$$\eta_t = \frac{4}{3}\eta \int dq d\Omega \frac{q^4}{(2\pi)^3} \frac{\gamma(q, \Omega)}{\Omega^2 + \eta^2 q^4}. \tag{50}$$

Note that there are instances where the expression for the diffusivity cannot be valid on all lengthscales, though these are not physically realistic scenarios. Consider for example the simple case where $\gamma(q, \Omega)$ is a constant. In this case, the integral (50) diverges. This does not mean that there is an issue with expression (50), rather that this expression cannot be applicable to all scales, and there must be a wavenumber at which the integral is cut off. At very large wavenumbers the theory cannot possibly capture the dominant physics, as we would be considering lengthscales smaller than the size of an atom (and our theory is not quantum mechanical).

In the following section, we compare our results to those of previous studies which considered the same problem by different means.

VI. COMPARISON TO LITERATURE AND PHYSICAL IMPLICATIONS

Our expression for the turbulent diffusivity under the assumption of isotropic turbulence (50) may be compared to well-established literature. In particular, we will compare our result to those of Moffatt [32] and Kazantsev [23], who provided estimates of the turbulent diffusivity that might be expected in the case of isotropic turbulence in a conductive fluid. Moffatt computed an expression for the turbulent diffusivity via the mean-field theory framework developed by Steenbeck, Krause and Rädler [51], and found

$$\eta_t = \frac{2}{3}\eta \int dq d\Omega \; \frac{q^2 E(q, \Omega)}{\Omega^2 + \eta^2 q^4}, \tag{51}$$

where $E(q, \Omega)$ is defined as the energy spectrum function, such that

$$\int dq d\Omega \; E(q, \Omega) = \frac{1}{2}\langle \mathbf{u}^2 \rangle. \tag{52}$$

Physically, $\rho\langle\mathbf{u}^2\rangle/2$ is the kinetic energy density, where ρ is the fluid's density. Taking into account Moffatt's different definition of the Fourier transform, we may relate $E(q,\Omega)$ to $\gamma(q,\Omega)$ via

$$E(q,\Omega) = \frac{2q^2\gamma(q,\Omega)}{(2\pi)^3}. \tag{53}$$

Plugging (53) into (51) reveals that our estimate of η_t is identical to that proposed by Moffatt using mean-field theory. The agreement between our results and Moffatt's at this stage is perhaps not too surprising. The first-order smoothing approximation used in mean-field theory is analogous to the Born approximation in scattering theory [32]. Our first order expression for the Green function (39) is exactly the Born approximation in the language of scattering theory. This agreement also lends credence to the assumption of a Gaussian probability distribution for the velocity (at least in studying this specific problem), as Moffatt does not make any assumptions about the velocity's statistics. Though it may appear more laboured, the advantage of our method is that it can be extended to include an infinite number of terms in the perturbation series by exploiting the field theory formalism.

Let us now compare our results to Kazantsev's study. Kazantsev developed a model for the turbulent motion of a conductive fluid, assuming that the fluid flow has a Gaussian distribution function and is delta-correlated in time. This problem's set-up is very similar to our own, though Kazantsev works directly with the magnetic field (rather than the magnetic vector potential), and imposes solenoidality through the enforcement of initial conditions. By establishing a recursive relation for the magnetic field's Green function, he was able to extract an expression for the turbulent diffusivity contribution of the form

$$\eta_t = \frac{1}{3}\int dq\ q^2\frac{\gamma(q)}{(2\pi)^3}, \tag{54}$$

where $\gamma(q)$ is now purely a function of wavevector. This result may be readily derived from (50) by taking the velocity to be delta-correlated in time. Moffatt and Kazantsev's estimates may be thought of as being valid in different limits of a *turbulent* magnetic Reynolds number, Rm^t. This non-dimensional parameter quantifies the relative strength of the inductive and advective effects due to the turbulent velocity fluctuations compared to magnetic diffusion, and is defined by

$$Rm^t = \frac{\ell^2}{\eta\tau}, \tag{55}$$

where τ and ℓ are the velocity's correlation time and length respectively. This magnetic Reynolds number refers specifically to the fluctuating part of the velocity. Kazantsev's assumption of instantaneous time correlation requires τ to be small compared to the diffusive timescale ℓ^2/η. The inequality $\tau \ll \ell^2/\eta$ may be recast as $Rm^t \gg 1$, suggesting that Kazantsev's result is the high Rm^t limit of Moffatt's more general result (51).

The geodynamo is thought to operate at a global $Rm \sim 1000$ [52] (based on the average velocity scale), though scale separation makes it more appropriate to consider a local Rm^t when considering turbulent processes. If the turbulent flow's lengthscale were to correspond to the dissipation lengthscale, Rm^t could be as low as $Rm^t \sim 1$ [13]. Holdenried-Chernoff and Buffett [46] found that a local Rm^t based on the eddy dissipation lengthscale might be an order of magnitude smaller than the global Rm, so we might expect $Rm^t < 100$ at the lengthscales relevant to the turbulent flow. These are quite moderate values, so if we wanted to consider the turbulent diffusivity in the context of the geodynamo we should probably use the more general expression (50). However, this involves the correlation function $\gamma(q,\Omega)$, which is unknown for velocity correlations in the Earth. As an illustrative example, let us assume that the velocity is exponentially correlated in both space and time, such that

$$\langle\mathbf{u}(\mathbf{x},t)\cdot\mathbf{u}(\mathbf{x}',t')\rangle = u_{\text{rms}}^2 e^{-|\mathbf{x}-\mathbf{x}'|/\ell}e^{-|t-t'|/\tau}. \tag{56}$$

Here, u_{rms} is the average root mean square velocity in the outer core. In conjunction with (50), this correlation function yields a turbulent diffusivity

$$\eta_t = \frac{1}{3}u_{\text{rms}}^2\tau\left(1 + \sqrt{\frac{\eta\tau}{\ell^2}}\right)^{-2}, \tag{57}$$

where last term in brackets corresponds to $(Rm^t)^{-1/2}$. In the $\tau \to 0$ (short correlation time) or $\eta \to 0$ (high Rm^t) limit, this expression corresponds to the relation derived by Holdenried-Chernoff and Buffett [46] using mean-field theory, namely

$$\eta_t = \frac{1}{3}u_{\text{rms}}^2\tau. \tag{58}$$

Using (58) and estimates of the magnetic dipole's correlation times from paleomagnetic records, Holdenried-Chernoff and Buffett were able to compute an estimate for the average flow velocities expected in the outer core, and found that they were consistent with measurements of core surface velocities. Accounting for the effects of finite $Rm^t \gtrsim 1$, we might expect the estimate of u_{rms} to increase at most by a factor of 2.

VII. FORMAL EXTENSION TO ALL ORDERS

In sections IV B and V we computed the first order correction to the propagator and magnetic diffusivity. While this is a good first step towards understanding the effects of turbulence on the magnetic field's decay rate, it is only an approximation to the true turbulent diffusivity. Crucially, the results we have obtained so far require the amplitude of the velocity correlations, u_{rms}, to be small compared to the molecular diffusivity. To compute the full propagator we need to not only include the one vertex diagrams from the previous section, but also those with two vertices, three vertices and so on. We may improve our first order estimate of the turbulent diffusivity by including higher order diagrams in the limit of short fluid correlation times. We do this by using a technique pioneered by Dyson [53] to formally include all diagrams. This section illustrates the utility of formulating this problem as an interacting field theory; by borrowing its diagrammatic machinery, we can easily manipulate the perturbation series to express the propagator compactly in terms of a 'self-energy'. However, this is still written as a series expansion in powers of u_{rms}, so the manipulations are only helpful if the self-energy can be efficiently approximated. There are many possible ways of doing this depending on the particular structure of the theory; determining the best approach is often quite involved. Here we treat the case where the fluid correlation time is short, which results in a particularly simple expression for the self-energy.
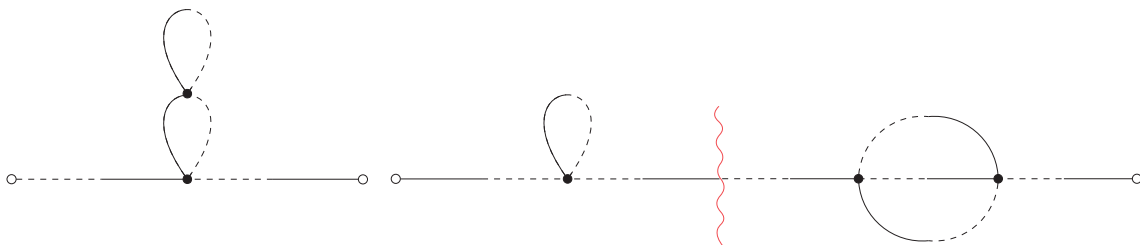

FIG. 4. The diagram on the left is 1PI, as cutting any internal line results in a physically meaningless diagram. The diagram on the right is $\overline{\text{1PI}}$, as it can be cut along the wavy red line to produce two 1PI diagrams.

Let us begin by separating the diagrams into two distinct types; those that are *one particle irreducible* (1PI) and those that are not ($\overline{\text{1PI}}$). The latter type can be split into two physically permissible diagrams by cutting one internal line, while in a 1PI diagram no internal line can be cut to produce a meaningful diagram. Figure 4 illustrates the difference between 1PI and $\overline{\text{1PI}}$ diagrams. From this example, it becomes clear that any $\overline{\text{1PI}}$ diagram may be built solely out of 1PI diagrams. The 1PI diagrams up to second order are

$$\tag{59}$$

Denoting the sum of all 1PI diagrams $\boldsymbol{\Xi}$, we may reorder the expansion for the propagator (written up to first order in (32)), so that it may be expressed diagrammatically as a geometric series, shown in Fig. 5. This is a standard procedure in many-body physics, with $\boldsymbol{\Xi}$ representing a self-energy. This Dyson series includes every single diagram, and so is an exact expression for the propagator. Since it is written as a geometric series, we may sum it to all orders. Let us call $\Gamma_{\psi\phi}(\mathbf{k}, \omega)$ the exact average, such that

$$\langle A_\psi(\mathbf{k}, \omega)\tilde{A}_\phi(\mathbf{k}', \omega')\rangle = (2\pi)^4 \delta(\mathbf{k} + \mathbf{k}')\delta(\omega + \omega')i\Gamma_{\psi\phi}(\mathbf{k}, \omega). \tag{60}$$

The interaction cannot affect the spatial and time translation invariance of the system, which is why we have delta functions on the wavevectors and frequencies. Fig. 5 tells us that the magnetic potential's Green function ($i\Gamma_{\psi\phi}$) may be written to all orders as
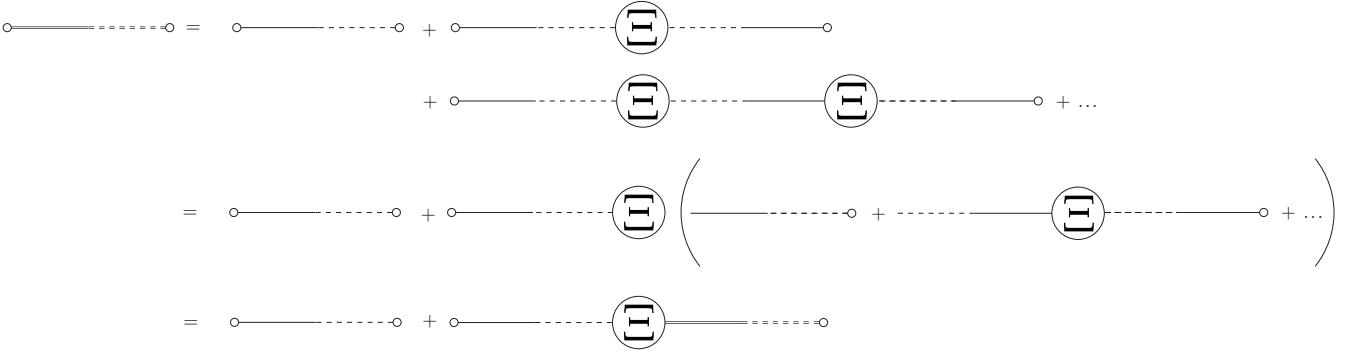
FIG. 5. Diagrammatic illustration of the expansion for the quantity $\langle \mathbf{A}(\mathbf{k},\omega)\tilde{\mathbf{A}}(\mathbf{k}',\omega')\rangle$. The exact average is represented by double lines, where the solid and dashed lines indicate $\mathbf{A}$ and $\tilde{\mathbf{A}}$ respectively. The first diagram on the right-hand side is the purely diffusive, zero-order contribution to the average. Higher order contributions may be written in 1PI form, with each higher order having an additional Ξ contribution (Ξ is the sum of all 1PI diagrams). The exact propagator may be expressed as a geometric series, where each subsequent term includes an additional Ξ contribution.

$$\boldsymbol{\Gamma}(\mathbf{k},\omega) = \mathbf{G}(\mathbf{k},\omega) \cdot \sum_{n=0}^{\infty} (-\boldsymbol{\Xi}(\mathbf{k},\omega) \cdot \mathbf{G}(\mathbf{k},\omega))^n = \mathbf{G}(\mathbf{k},\omega) \left(\mathbf{1} + \boldsymbol{\Xi}(\mathbf{k},\omega) \cdot \mathbf{G}(\mathbf{k},\omega)\right)^{-1}, \tag{61}$$

where $\mathbf{1}$ is the identity matrix. The matrix $\mathbf{G}(\mathbf{k},\omega)$ is a shorthand for the zero order contribution

$$\mathbf{G}(\mathbf{k},\omega) = g_0(\mathbf{k},\omega)\mathbf{1}. \tag{62}$$

The solution for $\boldsymbol{\Gamma}(\mathbf{k},\omega)$ in (61) is formally exact, although computing $\boldsymbol{\Xi}(\mathbf{k},\omega)$ exactly is an intractable problem. To make progress, we require a scheme for approximating $\boldsymbol{\Xi}(\mathbf{k},\omega)$. This can be done perturbatively, by systematically increasing the number of vertices in the diagrams, but ultimately this series is only likely to be accurate for small u_{rms}. Alternatively, we may look at the diagrams' contributions in a limit that is independent of the velocity fluctuations' size, for example in the case that the velocity's time correlation is short. In this limit, only finitely many diagrams make a significant contribution to $\boldsymbol{\Xi}(\mathbf{k},\omega)$. Every 1PI diagram contains integrals over the momenta and frequencies that run around its loops. Their corresponding integrands contain combinations of propagators and velocity correlations. If the velocity has a very short correlation time, the size of the integrals is controlled by the behaviour of the integrand at high frequency. Since each propagator's decay is inversely proportional to the frequency in this limit, the 1PI diagrams' contribution diminishes as the number of propagators they contain increases (such as for the second order diagrams in (59)). The first order 1PI contribution involves the fewest propagator factors, so it is justifiable to keep only the first order loop and its derivative $\overline{1\text{PI}}$ diagrams in the expansion for $\boldsymbol{\Xi}(\mathbf{k},\omega)$

$$\tag{63}$$

Leaving the details of this calculation to Appendix E, we compute an expression for the magnetic field's Green function to all orders in the loop diagram, and find

$$\mathcal{G}_{\alpha\beta}(\mathbf{k},\omega) = \frac{\sigma_{\alpha\beta}(\mathbf{k})}{g_0^{-1}(\mathbf{k},\omega) + \Xi(\mathbf{k},\omega)}, \tag{64}$$

where

$$\Xi(\mathbf{k},\omega) = \frac{1}{2}\int d\!\!\!/\mathbf{q}\, d\!\!\!/\Omega\, \gamma(\mathbf{q},\Omega)\big[g_0(\mathbf{k}-\mathbf{q},\omega-\Omega) + g_0(\mathbf{k}+\mathbf{q},\omega+\Omega)\big]\left(k^2 - \frac{1}{q^2}(\mathbf{k}\cdot\mathbf{q})^2\right). \tag{65}$$

Eq. (64) allows us to compute the influence of the additional loop diagrams on the effective diffusivity. Following the same procedure as in section V, we find that the diffusivity remains unchanged compared to (50). Note that g^{-1} is

no longer approximated by (46), as it is exactly given by the denominator of (64). This appears to be equivalent to the calculation that Kazantsev [23] illustrates in Fig. 2 of his paper.

While we have formally neglected an infinite number of contributions, the infinity of diagrams based on the first order loop that we do consider agrees exactly with mean-field theory, which has been shown to be very successful [24, 32] as long as the velocity's correlation time is small. The advantage of using the field theory approach is that the treatment may be extended to consider longer correlation times. In the core, the velocity's correlation time has been estimated to be of order $\sim 10^2$ years [46], which is relatively short compared to the magnetic field's decay timescale (which can be as long as $\sim 10^4$ years for the dipole), so the results derived for short correlation times may be sufficient.

Even though we have only considered Ξ in the limit of small time correlations, this scheme always contains more information than naive perturbation theory, as we are no longer restricting the velocity to have small amplitudes. Computing the contributions from the higher order diagrams is necessary when longer correlation times are considered. In this regime, we would expect the results for the turbulent diffusivity to change, as these diagrams alter the propagator's properties (wavenumber and index structure) compared to the results given here. The next order in Ξ must include all 1PI contributions with two vertices, although the hope is that one of the second order diagrams will dominate, so that the self-energy can be effectively approximated. We leave this to future work, as the principle aim of this paper is to introduce the MSRJD framework to the problem of studying stochastic dynamos.

VIII.   CONCLUSIONS

Studying the induction equation in the framework of stochastic models appears to be a reasonable way of understanding the long timescale behaviour of the Earth's magnetic field. A theoretical understanding of this behaviour can be coupled with statistical information extracted from paleomagnetic records to infer properties of the fluid flow underlying the geodynamo.

We have introduced methods commonly used in field theory to create a framework that allows us to compute ensemble averages of arbitrary observables of the magnetic field. By computing the magnetic field's average Green function, we find an expression for the turbulent magnetic diffusivity that is exactly consistent with the results of Moffatt's [32] mean-field theory estimate. The turbulent contribution to the diffusivity is positive (and thus enhances the magnetic field's decay), and depends on the spatio-temporal correlation function of the velocity. Our results are also consistent with Kazantsev's [23] study when the velocity is restricted to be delta-correlated in time. The methods applied in this paper allow us to compute arbitrary observables of the magnetic field in the limit of short velocity correlation times.

Taking the high Rm limit results in a relation between the turbulent diffusivity and the average root mean squared velocity in the bulk of the fluid. Making use of this expression along with an estimate of the turbulent diffusivity in the Earth from paleomagnetic constraints, Holdenried-Chernoff and Buffett [46] found an upper bound on the possible average fluid velocities in the outer core. This estimate is consistent with measured core surface flows, suggesting that although both mean-field theory and our approach make a number of simplifying assumptions compared to the true Earth system, they should at least be capturing the turbulent effects' correct order of magnitude.

In principle, we could restrict our calculation to spherical geometry by imposing the velocity's correlations to go to zero outside the sphere's radius. While the change in geometry would most probably have some quantifiable impact on the expressions we have derived, it should not drastically alter the system's physics (and consequently the expressions' qualitative structure), though it would restrict the set of velocities that we should consider when averaging.

In this study we have looked specifically at the diffusivity. Equally, we could have considered the stochastic velocity's effect on other processes, such as magnetic induction through the alpha effect. This is captured by terms that are independent of k in the frequency pole of the magnetic field's Green function. To examine these inductive effects we would need to see how the coefficients of $\mathbf{B}$ terms are altered (in the purely diffusive case these coefficients are of course zero). The particular set-up that we have chosen does not support an alpha effect, as the velocity's correlations are symmetric upon reflection. The alpha effect is intrinsically linked to the fluid's helicity, which requires the system to have a lower symmetry than we have imposed. Our model may be extended to account for this by using the more general velocity correlation function given in (18).

The great advantage of employing the MSRJD method for studying this problem is that it unlocks a wealth of powerful field theory techniques that may be used to take the problem further. For example, the work presented here could form the basis for a perturbative momentum shell renormalization group, where small scale velocity and magnetic field fluctuations are integrated out to obtain an effective theory valid for fluctuations on longer lengthscales. This opens the possibility of determining critical exponents or effect values for coupling constants valid for a given lengthscale in the theory.

We emphasise that this paper only treats the simplest case, and we have only extracted one piece of information (the turbulent diffusivity) from the system. However, we believe that applying field-theory methods to the stochastic

induction equation has great potential for addressing a number of interesting questions. For example, if we were to introduce a mean fluid velocity that acts as a kinematic dynamo, we could ask how the stochastic motions affect the fluid's ability to induce magnetic field, and investigate whether turbulence is beneficial or detrimental to sustaining the dynamo. Ultimately, the greatest flaw in our model is the need to assume the form of the velocity's probability distribution. The final goal in stochastic geodynamo studies should be to develop a fully self-consistent model that accounts for the Navier-Stokes equation as well as the induction equation.

ACKNOWLEDGMENTS

DATA AVAILABILITY STATEMENT

No new data were created or analysed in this study.

Appendix A: Detailed derivation of MSRJD action

This appendix provides a step-by-step explanation of the MSRJD procedure used to derive the actions in (14). Our aim is to compute observables of the magnetic field given (2) and the statistics of $\mathbf{u}$, subject to the constraint (3). The latter constraint may be enforced by expressing the magnetic field in terms of the magnetic vector potential $\mathbf{A}(\mathbf{x}, t)$, such that $\mathbf{B} = \nabla \times \mathbf{A}$. Written in terms of $\mathbf{A}$, the induction equation (2) becomes

$$\frac{\partial \mathbf{A}}{\partial t} = \mathbf{u} \times (\nabla \times \mathbf{A}) + \eta \nabla^2 \mathbf{A} + \nabla \chi, \tag{A.1}$$

where χ is an arbitrary scalar. This scalar may be set to zero, effectively absorbing it into the gauge function for $\mathbf{A}$. The magnetic vector potential's gauge is set through the Faddeev-Popov procedure (see Appendix C). Complete information on the magnetic vector potential's statistics will allow us to compute any magnetic field statistics.

Let us begin by considering how to compute the expectation value of an observable $\langle O[\mathbf{A}] \rangle$. This will in general be a functional of $\mathbf{A}$, most commonly consisting of a combination of products of $\mathbf{A}$ and/or its derivatives at various points in space and time. For example, one of the most common observables to consider is the auto-correlation

$$\langle \mathbf{A}_i(\mathbf{x}_1, t_1) \mathbf{A}_j(\mathbf{x}_2, t_2) \rangle,$$

while an example of a more complex observable is the expectation value of the magnetic field's helicity

$$\langle (\nabla \times \mathbf{A}(\mathbf{x}, t)) \cdot (\nabla \times \nabla \times \mathbf{A}(\mathbf{x}, t)) \rangle.$$

Evaluating these averages requires knowledge of the probability of finding a particular function $\mathbf{A}$ at all points in space and time. This can be done by using functional methods borrowed from field theory. We will employ these methods without providing their proofs (which can be found in [48–50]), though we will physically motivate their use.

It is easiest to begin by considering the problem under a discrete representation. Suppose that we split time into a discrete set of points t_i labelled by an index "i". The points t_i and t_{i-1} are separated by an interval Δt, which vanishes in the continuous limit. Denoting the magnetic vector potential at each point $\mathbf{A}_i \equiv \mathbf{A}(\mathbf{x}, t_i)$, we may write the expectation value of an observable as

$$\langle O\left[\{\mathbf{A}_i\}\right] \rangle = \frac{\int \prod_i d\mathbf{A}_i \, O[\{\mathbf{A}_i\}] \langle p[\{\mathbf{A}_i\} | \{\mathbf{u}\}] \rangle}{\int \prod_i d\mathbf{A}_i \, \langle p[\{\mathbf{A}_i\} | \{\mathbf{u}_i\}] \rangle}, \tag{A.2}$$

where $\{\mathbf{A}_i\}$ and $\{\mathbf{u}_i\}$ denote the set of all $\mathbf{A}_i$ and $\mathbf{u}_i$ respectively. The probability of obtaining the set of all possible realisations of the vector potential, given all possible velocity realisations, is written $\langle p[\{\mathbf{A}_i\}|\{\mathbf{u}_i\}]\rangle$. The denominator is simply the probability distribution's normalisation. In the continuous limit, (A.2) becomes

$$\langle O[\mathbf{A}] \rangle = \frac{\int \mathcal{D}\mathbf{A} \ O[\mathbf{A}] \langle p[\mathbf{A}|\mathbf{u}] \rangle}{\int \mathcal{D}\mathbf{A} \ \langle p[\mathbf{A}|\mathbf{u}] \rangle}, \tag{A.3}$$

where $\int \mathcal{D}\mathbf{A}$ denotes a functional (path) integral over all possible $\mathbf{A}(\mathbf{x}, t)$ and $p[\mathbf{A}|\mathbf{u}]$ is the functional probability distribution of $\mathbf{A}$ given $\mathbf{u}$. For the moment, let us return to the discrete representation of eq. (A.2). The average of the probability distribution is

$$\langle p[\{\mathbf{A}_i\}|\{\mathbf{u}_i\}] \rangle = \frac{\int \prod_i d\mathbf{u}_i \ p[\{\mathbf{u}_i\}] \ p[\{\mathbf{A}_i\}|\{\mathbf{u}_i\}]}{\int \prod_i d\mathbf{u}_i \ p[\{\mathbf{u}_i\}]}. \tag{A.4}$$

For simplicity, the probability distribution for $\mathbf{u}_i$ is taken to be Gaussian and is given in eq. (4). The probability $p[\{\mathbf{A}_i\}|\{\mathbf{u}_i\}]$ requires that for any given $\mathbf{u}_i$, $\mathbf{A}_i$ must both solve the induction equation and satisfy the appropriate boundary conditions at each point in space and time. Denoting the $\mathbf{A}_i$ that solves (A.1) as $\mathbf{A}_i^*(\{\mathbf{u}_i\})$, we may write

$$p[\{\mathbf{A}_i\}|\{\mathbf{u}_i\}] = \prod_i \delta[\mathbf{A}_i - \mathbf{A}_i^*(\{\mathbf{u}_i\})], \tag{A.5}$$

that is the probability of observing $\mathbf{A}_i$ for a given realisation of $\mathbf{u}_i$ is a delta-function on solutions to (A.1). In continuous notation, this is simply

$$p[\mathbf{A}|\mathbf{u}] = \delta[\mathbf{A} - \mathbf{A}^*(\mathbf{u})]. \tag{A.6}$$

Rather than solving for $\mathbf{A}^*(\mathbf{u})$, it is more convenient to transform to a new variable, $\mathbf{X}$, that represents (A.1). Using a discrete representation, we have

$$\mathbf{X}_i = \frac{1}{\Delta t}\big(\mathbf{A}(\mathbf{x}, t_i) - \mathbf{A}(\mathbf{x}, t_{i-1})\big) - \mathbf{u}(\mathbf{x}, t_{i-1}) \times \nabla \times \mathbf{A}(\mathbf{x}, t_{i-1}) - \eta \nabla^2 \mathbf{A}(\mathbf{x}, t_{i-1}). \tag{A.7}$$

Note that $\mathbf{X} = \mathbf{0}$ when $\mathbf{A} = \mathbf{A}^*(\mathbf{u})$. Making use of the standard property of delta-functions, (A.5) becomes

$$p[\{\mathbf{A}_i\}|\{\mathbf{u}_i\}] = \left|\frac{\partial \mathbf{X}_j}{\partial \mathbf{A}_k}\right| \prod_i \delta[\mathbf{X}_i]. \tag{A.8}$$

In continuous notation, we have

$$p[\mathbf{A}|\mathbf{u}] = \left|\frac{\delta \mathbf{X}}{\delta \mathbf{A}}\right| \delta[\mathbf{X}]. \tag{A.9}$$

The Jacobian matrix $\partial \mathbf{X}_j/\partial \mathbf{A}_k$ is triangular, so its determinant equals the product of its diagonal elements. In this case, it is simple to show that $\left|\partial \mathbf{X}_j/\partial \mathbf{A}_k\right| \propto 1/(\Delta t)^N$. Since the determinant does not depend on $\mathbf{A}_i$ or $\mathbf{u}_i$, only on the choice of discretization, any constant values will cancel out with the probability distribution's normalisation once we take the averages required for (A.2). To make progress, we may write the delta function in terms of its Fourier transform. In one dimension we have

$$\delta(x - a) = \int đk \ e^{ik(x-a)}, \tag{A.10}$$

which becomes

$$\prod_i \delta(\mathbf{X}_i) = \int \prod_i đ\tilde{\mathbf{A}}_i \exp\left[i \sum_i \tilde{\mathbf{A}}_i \cdot \mathbf{X}_i\right] \tag{A.11}$$

in the discrete case. Passing back to the continuous representation, we may write the probability distribution as

$$p[\mathbf{A}|\mathbf{u}] \propto \delta\left[\frac{\partial \mathbf{A}}{\partial t} - \mathbf{u} \times (\nabla \times \mathbf{A}) - \eta \nabla^2 \mathbf{A}\right]$$
$$\propto \int \mathcal{D}\tilde{\mathbf{A}} \exp\left[i \int d\mathbf{x} \ dt \ \tilde{\mathbf{A}} \cdot \left(\frac{\partial \mathbf{A}}{\partial t} - \mathbf{u} \times (\nabla \times \mathbf{A}) - \eta \nabla^2 \mathbf{A}\right)\right] \tag{A.12}$$

where the normalisation has not explicitly been written, and $\tilde{\mathbf{A}}(\mathbf{x}, t)$ is the "conjugate field" to $\mathbf{A}(\mathbf{x}, t)$ [48]. The exponent's argument is integrated over time and space. This can be understood by considering the discrete representation of the field; at every spatio-temporal point $(\mathbf{x}, t)$, each realisation of $\mathbf{A}(\mathbf{x}, t)$ has an associated $\tilde{\mathbf{A}}(\mathbf{x}, t)$. Summing over these realisations produces the integrals given in (A.12). To obtain the average of $p[\mathbf{A}|\mathbf{u}]$ over all realisations of $\mathbf{u}$ we take the continuous limit of (A.4),

$$\langle p[\mathbf{A}|\mathbf{u}]\rangle = \frac{\int \mathcal{D}\mathbf{u}\, p\,[\mathbf{u}]\, p\,[\mathbf{A}|\mathbf{u}]}{\int \mathcal{D}\mathbf{u}\, p\,[\mathbf{u}]}. \tag{A.13}$$

Combining (A.12), (A.13) and (4), we find

$$\langle O[\mathbf{A}]\rangle_u = \mathcal{N} \int \mathcal{D}\mathbf{A}\mathcal{D}\tilde{\mathbf{A}}\mathcal{D}\mathbf{u}\, O[\mathbf{A}] \exp\left[-\frac{1}{2} \int d\mathbf{x}\, d\mathbf{x}'\, dt\, dt'\, u_k C_{kj}^{-1} u_j \right.$$
$$\left. + i \int d\mathbf{x} dt \tilde{A}_j \left(\frac{\partial A_j}{\partial t} - u_k \varepsilon_{klj}(\nabla \times \mathbf{A})_l - \eta \nabla^2 A_j \right) \right], \tag{A.14}$$

where the fields' arguments have been kept implicit for notational clarity, and $\mathcal{N}$ is the normalisation constant. Note that repeated indices are summed over. Given the form of $p[\mathbf{u}]$, we may take the functional integral over the velocity by performing a Gaussian integral. We make use of the identity (see chapter 3 of [48])

$$\int \mathcal{D}\mathbf{u}\, \exp\left[-\frac{1}{2} \int d\mathbf{x} d\mathbf{x}' dt dt' \mathbf{u}(\mathbf{x}, t) \cdot \mathbf{C}^{-1}(\mathbf{x}, \mathbf{x}', t, t') \cdot \mathbf{u}(\mathbf{x}', t') - \int d\mathbf{x} dt\, \mathbf{h}(\mathbf{x}, t) \cdot \mathbf{u}(\mathbf{x}, t) \right]$$
$$= \det(2\pi\mathbf{C})^{1/2} \exp\left[\frac{1}{2} \int \int d\mathbf{x}\, d\mathbf{x}'\, dt\, dt'\, \mathbf{h}(\mathbf{x}, t) \cdot \mathbf{C}(\mathbf{x}, \mathbf{x}', t, t') \cdot \mathbf{h}(\mathbf{x}', t') \right], \tag{A.15}$$

to write (A.14) as

$$\langle O[\mathbf{A}]\rangle = \mathcal{N} \int \mathcal{D}\mathbf{A}\mathcal{D}\tilde{\mathbf{A}}\, O[\mathbf{A}] \exp\left[-S_0[\mathbf{A}, \tilde{\mathbf{A}}] - S_{\mathrm{int}}[\mathbf{A}, \tilde{\mathbf{A}}, \mathbf{C}] \right]. \tag{A.16}$$

Here we have introduced the action $S[\mathbf{A}, \tilde{\mathbf{A}}] = S_0[\mathbf{A}, \tilde{\mathbf{A}}] + S_{\mathrm{int}}[\mathbf{A}, \tilde{\mathbf{A}}, \mathbf{C}]$, where $S_0[\mathbf{A}, \tilde{\mathbf{A}}]$ (the "free action") is the contribution we would have from free decay (i.e. $\mathbf{u} = \mathbf{0}$), while $S_{\mathrm{int}}[\mathbf{A}, \tilde{\mathbf{A}}, \mathbf{C}]$ (the "interaction action") represents the interaction part obtained by integrating over all possible representations of $\mathbf{u}$. These are respectively

$$S_0 = -i \int d\mathbf{x}\, dt\, \tilde{\mathbf{A}} \cdot \left(\partial_t \mathbf{A} - \eta \nabla^2 \mathbf{A} \right) = -i \int d\mathbf{x}\, dt\, \tilde{\mathbf{A}}(\mathbf{x}', t') \cdot g_0^{-1}(\mathbf{x}, \mathbf{x}', t, t') \cdot \mathbf{A}(\mathbf{x}, t), \text{ and}$$
$$S_{\mathrm{int}} = \frac{1}{2} \int d\mathbf{x}\, d\mathbf{x}'\, dt\, dt' \left[\varepsilon_{jab}(\nabla \times \mathbf{A})_a(\mathbf{x}, t)\tilde{A}_b(\mathbf{x}, t)C_{jk}(\mathbf{x}, \mathbf{x}', t, t')\varepsilon_{kcd}(\nabla \times \mathbf{A})_c(\mathbf{x}', t')\tilde{A}_d(\mathbf{x}', t') \right]. \tag{A.17}$$

Note that the purely diffusive operator $\partial_t - \eta \nabla^2$ is written in terms of the inverse of its Green function, $g_0(\mathbf{x}, t)$.

Appendix B: Fourier transform of interaction term

The general, incompressible form of the probability distribution for the velocity in Fourier space is

$$p[\mathbf{u}] = \exp\left[-\frac{1}{2} \int d\!\!\!/\mathbf{q}\, d\!\!\!/\mathbf{q}'\, d\omega\, d\omega'\, u_j(\mathbf{q}, \omega)C_{jk}^{-1}(\mathbf{q}, \mathbf{q}', \omega, \omega')u_k(\mathbf{q}', \omega') \right], \tag{B.1}$$

where $C_{jk}^{-1}(\mathbf{q}, \mathbf{q}', t, t')$ is the inverse of the correlation

$$\langle u_j(\mathbf{q}, \omega)u_k(\mathbf{q}', \omega')\rangle = C_{jk}(\mathbf{q}, \mathbf{q}', \omega, \omega') = (2\pi)^4 \gamma(\mathbf{q}, \omega)\delta(\mathbf{q} + \mathbf{q}')\delta(\omega + \omega')\sigma_{jk}(\mathbf{q}). \tag{B.2}$$

The function $\gamma(\mathbf{q}, \omega)$ represents any spatial and temporal structure of the noise and $\sigma_{jk}(\mathbf{q})$ is defined in (18). To make use of (B.2), we want to express the probability distribution $p[\mathbf{A}, \tilde{\mathbf{A}}]$ in terms of Fourier variables. A simple way of doing this is to write each of the variables appearing in the definitions (14) in terms of their inverse Fourier transform.

Let us consider how this works for the interaction term S_{int}, restricting our attention to the spatial Fourier transform. Time dependence is kept implicit for clarity, though the Fourier transform in time follows in the same manner. From (14) we have

$$
\begin{aligned}
S_{\text{int}} = & \int d\mathbf{x}\, d\mathbf{x}' \int d\!\!\!{}^-\mathbf{q}_{1\to6}\, e^{i\mathbf{q}_{1\to3}\cdot\mathbf{x}} e^{i\mathbf{q}_{4\to6}\cdot\mathbf{x}'} \varepsilon_{jab}\varepsilon_{kcd}(-i\mathbf{q}_1 \times \mathbf{A}(\mathbf{q}_1))_a \tilde{A}_b(\mathbf{q}_2) C_{jk}(\mathbf{q}_3,\mathbf{q}_4)(-i\mathbf{q}_5 \times \mathbf{A}(\mathbf{q}_5))_c \tilde{A}_d(\mathbf{q}_6) \\
= & -(2\pi)^3 \int d\mathbf{x}\, d\mathbf{x}' \int d\!\!\!{}^-\mathbf{q}_{1\to6} e^{i\mathbf{q}_{1\to3}\cdot\mathbf{x}} e^{i\mathbf{q}_{4\to6}\cdot\mathbf{x}'} \varepsilon_{jab}\varepsilon_{kcd}\gamma(\mathbf{q}_3)\sigma_{jk}(\mathbf{q}_3)\delta(\mathbf{q}_3+\mathbf{q}_4)(\mathbf{q}_1 \times \mathbf{A}(\mathbf{q}_1))_a \tilde{A}_b(\mathbf{q}_2) \\
& \hspace{10cm} (\mathbf{q}_5 \times \mathbf{A}(\mathbf{q}_5))_c \tilde{A}_d(\mathbf{q}_6) \quad \text{(B.3)} \\
= & \int d\mathbf{x}\, d\mathbf{x}' \int d\!\!\!{}^-\mathbf{q}_{1\to3} d\!\!\!{}^-\mathbf{q}_{5\to6} e^{i\mathbf{q}_{1\to3}\cdot\mathbf{x}} e^{i(\mathbf{q}_5+\mathbf{q}_6-\mathbf{q}_3)\cdot\mathbf{x}'} \varepsilon_{jab}\varepsilon_{kcd}\gamma(\mathbf{q}_3)\sigma_{jk}(\mathbf{q}_3)(\mathbf{q}_1 \times \mathbf{A}(\mathbf{q}_1))_a \tilde{A}_b(\mathbf{q}_2) \\
& \hspace{10cm} (\mathbf{q}_5 \times \mathbf{A}(\mathbf{q}_5))_c \tilde{A}_d(\mathbf{q}_6).
\end{aligned}
$$

Note that we may write

$$
\int d\mathbf{x}\, e^{i(\mathbf{q}_1+\mathbf{q}_2+\mathbf{q}_3)\cdot\mathbf{x}} = (2\pi)^3\delta(\mathbf{q}_1+\mathbf{q}_2+\mathbf{q}_3), \text{ and } \int d\mathbf{x}'\, e^{i(\mathbf{q}_5+\mathbf{q}_6-\mathbf{q}_3)\cdot\mathbf{x}'} = (2\pi)^3\delta(\mathbf{q}_5+\mathbf{q}_6-\mathbf{q}_3). \quad \text{(B.4)}
$$

Using this property, and taking the integrals over $\mathbf{q}_3$ and $\mathbf{q}_6$, we obtain

$$
\begin{aligned}
S_{\text{int}} = -\int d\!\!\!{}^-\mathbf{q}_1 d\!\!\!{}^-\mathbf{q}_2 d\!\!\!{}^-\mathbf{q}_5\, \varepsilon_{jab}\varepsilon_{kcd}\gamma(-\mathbf{q}_1-\mathbf{q}_2)\sigma_{jk}(-\mathbf{q}_1-\mathbf{q}_2)(\mathbf{q}_1 \times \mathbf{A}(\mathbf{q}_1))_a \tilde{A}_b(\mathbf{q}_2) \\
(\mathbf{q}_5 \times \mathbf{A}(\mathbf{q}_5))_c \tilde{A}_d(-\mathbf{q}_1-\mathbf{q}_2-\mathbf{q}_5).
\end{aligned} \quad \text{(B.5)}
$$

For notational clarity, let us define the new variables:

$$
\mathbf{p} = \mathbf{q}_1, \qquad\qquad \mathbf{p}' = \mathbf{q}_5, \qquad\qquad \mathbf{q} = -\mathbf{q}_1 - \mathbf{q}_2. \qquad \text{(B.6)}
$$

Making use of these variables, (B.5) becomes:

$$
-\int d\!\!\!{}^-\mathbf{p}\, d\!\!\!{}^-\mathbf{p}'\, d\!\!\!{}^-\mathbf{q}\, \varepsilon_{jab}\varepsilon_{kcd}\gamma(\mathbf{q})\sigma_{jk}(\mathbf{q})(\mathbf{p} \times \mathbf{A}(\mathbf{p}))_a \tilde{A}_b(-\mathbf{p}-\mathbf{q})(\mathbf{p}' \times \mathbf{A}(\mathbf{p}'))_c \tilde{A}_d(\mathbf{q}-\mathbf{p}'). \qquad \text{(B.7)}
$$

More compactly, we can express

$$
S_{\text{int}} = -\frac{1}{2}\int d\!\!\!{}^-\mathbf{p}\, d\!\!\!{}^-\mathbf{p}'\, d\!\!\!{}^-\mathbf{q}\, A_\alpha(\mathbf{p})\tilde{A}_\beta(-\mathbf{p}-\mathbf{q})M^{kl}_{\alpha\beta\gamma\delta}(\mathbf{q})p_k p'_l A_\gamma(\mathbf{p}')\tilde{A}_\delta(\mathbf{q}-\mathbf{p}'), \qquad \text{(B.8)}
$$

where

$$
M^{kl}_{\alpha\beta\gamma\delta}(\mathbf{q}) = \big(\delta_{k\beta}\delta_{l\delta}\sigma_{\alpha\gamma}(\mathbf{q}) - \delta_{\alpha\beta}\delta_{l\delta}\sigma_{k\gamma}(\mathbf{q}) - \delta_{k\beta}\delta_{\gamma\delta}\sigma_{\alpha l}(\mathbf{q}) + \delta_{\alpha\beta}\delta_{\gamma\delta}\sigma_{kl}(\mathbf{q})\big)\gamma(\mathbf{q}). \qquad \text{(B.9)}
$$

We may follow exactly the same procedure to Fourier transform in time. Reintroducing the time dependence, we find the interaction action to be of the form

$$
S_{\text{int}} = -\frac{1}{2}\int d\!\!\!{}^-\mathbf{p}\, d\!\!\!{}^-\mathbf{p}'\, d\!\!\!{}^-\mathbf{q}\, d\!\!\!{}^-\omega\, d\!\!\!{}^-\omega'\, d\!\!\!{}^-\Omega\, A_\alpha(\mathbf{p},\omega)\tilde{A}_\beta(-\mathbf{p}-\mathbf{q},-\omega-\Omega)M^{kl}_{\alpha\beta\gamma\delta}(\mathbf{q},\Omega)p_k p'_l A_\gamma(\mathbf{p}',\omega')\tilde{A}_\delta(\mathbf{q}-\mathbf{p}',\Omega-\omega'), \quad \text{(B.10)}
$$

where ω, ω' and Ω are Fourier conjugate frequencies and the Ω dependence in $M^{kl}_{\alpha\beta\gamma\delta}(\mathbf{q},\Omega)$ is entirely encapsulated by $\gamma(\mathbf{q},\Omega)$.

Appendix C: Gauge fixing term

It is worthwhile considering the system's dependence on the choice of gauge. A general observable of $\mathbf{B}$ may be written

$$
\langle B_{a_1}(\mathbf{q}_1,\omega_1)\dots B_{a_n}(\mathbf{q}_n,\omega_n)\rangle = i^n(\varepsilon_{a_1 b_1 c_1}q_1^{b_1})\dots(\varepsilon_{a_n b_n c_n}q_n^{b_n})\langle A_{c_1}(\mathbf{q}_1,\omega_1)\dots A_{c_n}(\mathbf{q}_n,\omega_n)\rangle. \qquad \text{(C.1)}
$$

All observables of $\mathbf{B}$ are gauge invariant, so we expect the RHS of (C.1) to also be gauge invariant. The cross products with $\mathbf{q}$ remove $\mathbf{A}$'s gauge dependence, which means that we require $p[\mathbf{A}, \tilde{\mathbf{A}}]$ to also be gauge invariant. Given that

$p[\mathbf{A}, \tilde{\mathbf{A}}]$ must be gauge invariant, it is possible to transform to a situation where $\mathbf{A} = 0$, so that we get an infinite number of constant integrals that lead to a poorly defined average [49]. To avoid this problem, it is necessary to fix $\mathbf{A}$'s gauge. We may turn to the Faddeev-Popov trick [54], commonly used when considering functional integrals of the electromagnetic field. A comprehensive discussion of this procedure may be found in section 9.4 of [49]. This trick leads to the introduction of the term

$$\exp\left[-\frac{i}{2g}\int d\mathbf{x}\, dt (\nabla \cdot \mathbf{A})^2\right] \tag{C.2}$$

to the probability (A.12), where g is a constant that determines the gauge. As fluid flows in Earth's core are on the order of ~ 1 mm s^{-1}, the system is non-relativistic, and the pre-Maxwell equations of electromagnetism are used. Neglecting the displacement current means that the electric field plays a secondary role compared to the magnetic field, and can be entirely determined from knowledge of the magnetic field. It is therefore sufficient to set the gauge of $\mathbf{A}$ without worrying about the electrostatic potential. The MSRJD procedure outlined in appendix A remains unaffected by the addition of the gauge fixing term in the exponent; the only difference is that S_0 is now defined as

$$S_0[\mathbf{A}, \tilde{\mathbf{A}}] = -i \int d\mathbf{x}\, dt\, \tilde{\mathbf{A}} \cdot g_0^{-1} \cdot \mathbf{A} + \frac{i}{2g} \int d\mathbf{x}\, dt\, (\nabla \cdot \mathbf{A})^2, \tag{C.3}$$

where the second term in the expression for S_0 is the gauge fixing term (C.2).

It is important to ensure that the addition of the gauge fixing term (C.2) to the free decay action does not affect any of the magnetic field observables. For notational clarity, we keep time dependence implicit throughout this appendix. Let us consider once again the expectation value of an observable $O[\mathbf{A}]$. Computing the integral over $\mathbf{A}$ and $\tilde{\mathbf{A}}$ is relatively easy for $S_0[\mathbf{A}, \tilde{\mathbf{A}}]$, since its form is Gaussian. This is not true for the interaction term. To make progress, we may expand $e^{-S_{\text{int}}}$ as a Taylor series, so the observable $\langle \mathbf{A}(\mathbf{q}) \rangle$ may be written to first order as

$$\langle A(\mathbf{q}) \rangle = \int \mathcal{D}\mathbf{A}\mathcal{D}\tilde{\mathbf{A}}\, A(\mathbf{q})e^{-S_0[\mathbf{A}, \tilde{\mathbf{A}}]}\left[1 - S_{\text{int}}[\mathbf{A}, \tilde{\mathbf{A}}, \mathbf{C}]\right] + O(S_{\text{int}}^2). \tag{C.4}$$

A general observable of $\mathbf{B}$ may be computed via

$$\langle \mathbf{B}(\mathbf{q}_1) \dots \mathbf{B}(\mathbf{q}_n) \rangle = \int \mathcal{D}\mathbf{A}\mathcal{D}\tilde{\mathbf{A}}\left(\mathbf{q}_1 \times \mathbf{A}(\mathbf{q}_1) \dots \mathbf{q}_n \times \mathbf{A}(\mathbf{q}_n)\right)e^{-S_0[\tilde{\mathbf{A}}, \mathbf{A}]}\left[1 - S_{\text{int}}[\mathbf{A}, \tilde{\mathbf{A}}]\right] \tag{C.5}$$

Given that the probability distribution for $\mathbf{u}$ is Gaussian, we may apply Wick's theorem, which states that

$$\left\langle \prod_{i=1}^{\ell} \mathbf{A}_i(\mathbf{q}_i) \right\rangle = \begin{cases} 0 & \ell \text{ odd,} \\ \text{sum over pairwise contractions} & \ell \text{ even.} \end{cases} \tag{C.6}$$

Using Wick's theorem we may consider purely pairwise correlations, since we are able to express any observable in terms of them. This means that we need only consider the following three pairwise correlations to ensure that the gauge fixing term has no effect on the correlations of physical observables (since the variables commute):

$$\langle \tilde{\mathbf{A}}(\mathbf{q})\tilde{\mathbf{A}}(\mathbf{q}') \rangle, \qquad\qquad \langle \tilde{\mathbf{A}}(\mathbf{q})\mathbf{A}(\mathbf{q}') \rangle, \qquad\qquad \langle \mathbf{A}(\mathbf{q})\mathbf{A}(\mathbf{q}') \rangle. \tag{C.7}$$

Written in matrix form, the action $S_0[\mathbf{A}, \tilde{\mathbf{A}}]$ is

$$S_0[\mathbf{A}, \tilde{\mathbf{A}}] = \begin{pmatrix} A_\alpha & \tilde{A}_\alpha \end{pmatrix}\begin{pmatrix} \frac{i}{g}q_\alpha q_\beta & -ig_0^{-1}\delta_{\alpha\beta} \\ -ig_0^{-1}\delta_{\alpha\beta} & 0 \end{pmatrix}\begin{pmatrix} A_\beta \\ \tilde{A}_\beta \end{pmatrix}, \qquad \text{where} \quad \Gamma_{\alpha\beta}^{-1} = \begin{pmatrix} \frac{i}{g}q_\alpha q_\beta & -ig_0^{-1}\delta_{\alpha\beta} \\ -ig_0^{-1}\delta_{\alpha\beta} & 0 \end{pmatrix}, \tag{C.8}$$

recalling that $g_0^{-1}(k, \omega) = i\omega + \eta k^2$. We can now read off these pairwise correlations, given by

$$\langle A_\alpha A_\beta \rangle = 0, \qquad\qquad \langle A_\alpha \tilde{A}_\beta \rangle = ig_0\delta_{\alpha\beta}, \qquad\qquad \langle \tilde{A}_\alpha \tilde{A}_\beta \rangle = \frac{i}{g}g_0 q_\alpha q_\beta g_0. \tag{C.9}$$

Let us consider the lowest order case that contains the interaction term for the average

$$\langle \mathbf{B}_\alpha(\mathbf{k})\mathbf{B}_\beta(\mathbf{k}') \rangle = -\int \mathcal{D}\mathbf{A}\mathcal{D}\tilde{\mathbf{A}}\left(\mathbf{k} \times \mathbf{A}\right)_\alpha (\mathbf{k}' \times \mathbf{A})_\beta e^{-S_0[\tilde{\mathbf{A}}, \mathbf{A}]}$$
$$\left[1 + \frac{1}{2}\int d\mathbf{p} d\mathbf{p}' d\mathbf{q} A_\alpha(\mathbf{p})\tilde{A}_\beta(-\mathbf{p} - \mathbf{q})M_{\alpha\beta\gamma\delta}^{kl}(\mathbf{q})p_k p_l' A_\gamma(\mathbf{p}')\tilde{A}_\delta(\mathbf{q} - \mathbf{p}')\right]. \tag{C.10}$$

To show that no observable depends on the gauge, we attempt to construct one that does. This observable must therefore include the factor g. Using Wick's theorem, we may split any observable into a sum of products of pairwise averages (C.9). Those that depend on g must include at least one $\langle \tilde{A}_\alpha \tilde{A}_\beta \rangle$. Since any observable includes the average of an equal number of $\tilde{\mathbf{A}}$s and $\mathbf{A}$s, factoring out at least one $\langle \tilde{A}_\alpha \tilde{A}_\beta \rangle$ must leave an excess of $\mathbf{A}$s. No matter how the remaining pairings are constructed, we will always be left with at least one $\langle A_\alpha A_\beta \rangle$. From (C.9), this pairing vanishes, therefore any term in the observable that depends on g, and hence the gauge, must also vanish.

Appendix D: Calculating the first order diagrams

This appendix provides a detailed description of how the contributions from each first order diagram were calculated. Let us begin by computing the contribution to (32) from diagram I_α. Following our rules, we may write

$$
\begin{aligned}
I_\alpha = & \langle A_\psi(\mathbf{k}, \omega) \tilde{A}_\beta(-\mathbf{p} - \mathbf{q}, -\omega_1 - \Omega) \rangle \langle A_\gamma(\mathbf{p}', \omega_2) \tilde{A}_\phi(\mathbf{k}', \omega') \rangle \langle A_\alpha(\mathbf{p}, \omega_1) \tilde{\mathbf{A}}_\delta(\mathbf{q} - \mathbf{p}', \Omega - \omega_2) \rangle \\
= & -\frac{i}{2} \int d\mathbf{p} d\mathbf{p}' d\mathbf{q} d\omega_1 d\omega_2 d\Omega \; p_k p_l' M_{\alpha\psi\phi\alpha}^{kl}(\mathbf{q}, \Omega) \delta(\omega_1 + \Omega - \omega_2) \delta(\omega - \omega_1 - \Omega) \\
& \delta(\omega_2 + \omega') \delta(\mathbf{q} - \mathbf{p}' + \mathbf{p}) \delta(\mathbf{k} - \mathbf{p} - \mathbf{q}) \delta(\mathbf{p}' + \mathbf{k}') g_0(\mathbf{p}, \omega_1) g_0(\mathbf{k}, \omega) g_0(\mathbf{k}', \omega').
\end{aligned}
\tag{D.1}
$$

Taking the integrals over $\mathbf{p}$, $\mathbf{p}'$, ω_1 and ω_2 we find

$$
I_\alpha = -\frac{i}{2} \delta(\mathbf{k} + \mathbf{k}') \delta(\omega + \omega') g_0^2(\mathbf{k}, \omega) \int d\mathbf{q} d\Omega \; g_0(\mathbf{k} - \mathbf{q}, \omega - \Omega)(\mathbf{k} - \mathbf{q})_k k_l M_{\alpha\psi\phi\alpha}^{kl}(\mathbf{q}, \Omega),
\tag{D.2}
$$

where

$$
M_{\alpha\psi\phi\alpha}^{kl}(\mathbf{q}) = \left(\delta_{\phi\psi} \delta_{il} \delta_{jk} - \delta_{i\phi} \delta_{l\psi} \delta_{jk} \right) \gamma(\mathbf{q}, \Omega) \sigma_{ij}(\mathbf{q}).
\tag{D.3}
$$

Let us consider the contributions arising from the two terms in (D.3) separately. The contribution from the first term is

$$
\delta_{\phi\psi} \delta_{il} \delta_{jk} (\mathbf{k} - \mathbf{q})_k k_l \; \gamma(\mathbf{q}, \Omega) \sigma_{ij}(\mathbf{q}) = \gamma(\mathbf{q}, \Omega) \left(k^2 - \frac{(\mathbf{q} \cdot \mathbf{k})^2}{q^2} \right) \delta_{\phi\psi},
\tag{D.4}
$$

while the second term is

$$
\delta_{i\phi} \delta_{l\psi} \delta_{jk} (\mathbf{k} - \mathbf{q})_k k_l \; \gamma(\mathbf{q}, \Omega) \sigma_{ij}(\mathbf{q}) = \gamma(\mathbf{q}, \Omega) k_\psi \sigma_{\phi j}(\mathbf{q}) (\mathbf{k} - \mathbf{q})_j.
\tag{D.5}
$$

The difference between these two terms is that (D.4) only includes diagonal terms, whereas (D.5) has off-diagonal elements. These corrections are for the response of the magnetic vector potential, not the magnetic field, so they will be used in (31) to find $\mathcal{G}_{\alpha\beta}(\mathbf{k}, \mathbf{k}', \omega, \omega')$. Since (31) includes terms of the form $\varepsilon_{\alpha l \phi} \varepsilon_{\beta n \psi} k_n' k_l$ (which represent cross products with $\mathbf{k}$), (D.5) cannot contribute to the magnetic field's Green function, as its cross product with $\mathbf{k}$ is zero. This is true in general, so any of the diagrams for which we have "free" components of k will vanish.

Let us now consider the contribution from the I_β diagram. Here we have

$$
\begin{aligned}
I_\beta = -\frac{i}{2} \int d\mathbf{p} d\mathbf{p}' d\mathbf{q} d\omega_1 d\omega_2 d\Omega \; & p_k p_l' M_{\alpha\alpha\psi\phi}^{kl}(\mathbf{q}, \Omega) \delta(-\Omega) \delta(\omega - \omega_2 + \Omega) \delta(\omega_2 + \omega') \\
& \delta(-\mathbf{q}) \delta(\mathbf{k} - \mathbf{p}' + \mathbf{q}) \delta(\mathbf{p}' + \mathbf{k}') g_0(\mathbf{p}, \omega_1) g_0(\mathbf{k}, \omega) g_0(\mathbf{k}', \omega'),
\end{aligned}
\tag{D.6}
$$

where

$$
M_{\alpha\alpha\psi\phi}^{kl}(\mathbf{q}, \Omega) = -2\gamma(\mathbf{q}, \Omega)(\delta_{l\phi} \sigma_{\psi k} - \delta_{\psi\phi} \sigma_{lk}),
\tag{D.7}
$$

so

$$
\begin{aligned}
I_\beta = i \int d\mathbf{p} d\mathbf{q} d\omega_1 d\Omega \; & p_k k_l' \gamma(\mathbf{q}, \Omega)(\delta_{l\phi} \sigma_{\psi k} - \delta_{\psi\phi} \sigma_{lk}) \delta(\omega + \omega' + \Omega) \delta(-\Omega) \\
& \delta(-\mathbf{q}) \delta(\mathbf{k} + \mathbf{k}' + \mathbf{q}) g_0(\mathbf{p}, \omega_1) g_0(\mathbf{k}, \omega) g_0(\mathbf{k}', \omega').
\end{aligned}
\tag{D.8}
$$

The entire diagram has a k_l' dependence, so it will not contribute to the Green function for the induction equation. The same is true for the contribution from the I_γ diagram,

$$I_\gamma = i \int d\mathbf{p}' d\mathbf{q} d\omega_2 d\Omega \ p_l' k_k' \gamma(\mathbf{q}, \Omega)(\delta_{l\phi}\sigma_{\psi k} - \delta_{\psi\phi}\sigma_{lk})\delta(\omega + \omega' - \Omega)\delta(\Omega)$$
$$\delta(\mathbf{q})\delta(\mathbf{k} + \mathbf{k}' - \mathbf{q})g_0(\mathbf{p}', \omega_2)g_0(\mathbf{k}, \omega)g_0(\mathbf{k}', \omega'). \tag{D.9}$$

The I_δ diagram contributes

$$I_\delta = -\frac{i}{2}G_0^2(\mathbf{k}, \omega)\delta(\mathbf{k} + \mathbf{k}')\delta(\omega + \omega') \int d\mathbf{q} d\Omega \ \gamma(\mathbf{q}, \Omega)g_0(\mathbf{k} + \mathbf{q}, \omega + \Omega) \left[\delta_{\psi\phi}\left(k^2 - \frac{(\mathbf{k} \cdot \mathbf{q})^2}{q^2}\right) - k_k(\mathbf{k} + \mathbf{q})_l \delta_{k\psi}\sigma_{\phi l}\right]. \tag{D.10}$$

Again, the off-diagonal term proportional to k_k does not contribute to the induction equation Green function. Overall, the interaction contribution to the vector potential's Green function is

$$G_{\psi\phi}^{int}(\mathbf{k}, \mathbf{k}', \omega, \omega') = -i\langle \mathbf{A}_\psi(\mathbf{k}, \omega)\tilde{\mathbf{A}}_\phi(\mathbf{k}', \omega')\rangle_{\text{int}} = -i\left(I_\alpha + I_\delta\right). \tag{D.11}$$

Using (31), (D.1) and (D.10), we finally find the induction equation's Green function to first order to be

$$\mathcal{G}_{\alpha\beta}(\mathbf{k}, \mathbf{k}', \omega, \omega') = \frac{(2\pi)^4}{k^2}\delta(\mathbf{k} + \mathbf{k}')\delta(\omega + \omega')\varepsilon_{\alpha l\phi}\varepsilon_{\beta n\psi}k_n k_l \delta_{\phi\psi}\left[\frac{-i^2}{i\omega + \eta k^2}\right.$$
$$\left. + \frac{i^2}{2(i\omega + \eta k^2)^2}\int d\mathbf{q} d\Omega \left(\frac{\gamma(\mathbf{q}, \Omega)}{i(\omega - \Omega) + \eta(\mathbf{k} - \mathbf{q})^2} + \frac{\gamma(\mathbf{q}, \Omega)}{i(\omega + \Omega) + \eta(\mathbf{k} + \mathbf{q})^2}\right)\left(k^2 - \frac{(\mathbf{q} \cdot \mathbf{k})^2}{q^2}\right)\right] \tag{D.12}$$

Making use of $\varepsilon_{\beta n\psi}\varepsilon_{\alpha l\phi}k_n k_l \delta_{\phi\psi} = k^2\sigma_{\alpha\beta}(k)$, we find that this is equivalent to

$$\mathcal{G}_{\alpha\beta}(\mathbf{k}, \mathbf{k}', \omega, \omega') = (2\pi)^4\delta(\mathbf{k} + \mathbf{k}')\delta(\omega + \omega')\sigma_{\alpha\beta}(k)g(k, \omega), \tag{D.13}$$

where $g(k, \omega)$ is defined as

$$g(k, \omega) = \frac{1}{i\omega + \eta k^2}\left[1 - \frac{1}{2}\int d\mathbf{q} d\Omega \frac{k^2 - q^{-2}(\mathbf{q} \cdot \mathbf{k})^2}{i\omega + \eta k^2}\left(\frac{\gamma(\mathbf{q}, \Omega)}{i(\omega - \Omega) + \eta(\mathbf{k} - \mathbf{q})^2} + \frac{\gamma(\mathbf{q}, \Omega)}{i(\omega + \Omega) + \eta(\mathbf{k} + \mathbf{q})^2}\right)\right]. \tag{D.14}$$

Appendix E: Magnetic field Green function for all loop orders

To calculate the all orders loop contribution to the propagator, we assume that the loops dominate over the other 1PI diagrams, and that this is true at all orders (i.e. that a string of n loops dominates over any other n-vertex diagram). This assumption holds for short time correlations. Taking Ξ to first order so that it only includes loop contributions, Fig. 5 tells us that the Green function ($i\Gamma_{\psi\phi}$) for $\mathbf{A}$, may be written as

$$i\Gamma_{\psi\phi}(\mathbf{k}, \mathbf{k}', \omega, \omega') = ig_0(\mathbf{k}, \omega)\delta(\mathbf{k} + \mathbf{k}')\delta(\omega + \omega')\delta_{\psi\phi}$$
$$- \frac{i}{2}\int d\mathbf{q} d\mathbf{p} d\mathbf{p}' d\omega_1 d\omega_2 d\Omega \ \delta(\mathbf{k} - \mathbf{p} - \mathbf{q})\delta(\mathbf{q} - \mathbf{p}' + \mathbf{p})\delta(\omega - \omega_1 - \Omega)$$
$$\delta(\Omega - \omega_2 + \omega_1)g_0(\mathbf{k}, \omega)g_0(\mathbf{p}, \omega_1)\Gamma_{\gamma\phi}(\mathbf{p}', \mathbf{k}', \omega_2, \omega')\delta_{\psi\beta}\delta_{\alpha\delta}p_k p_l' M_{\alpha\beta\gamma\delta}^{kl}(\mathbf{q}, \Omega) \tag{E.1}$$
$$- \frac{i}{2}\int d\mathbf{q} d\mathbf{p} d\mathbf{p}' d\omega_1 d\omega_2 d\Omega \ \delta(\mathbf{k} - \mathbf{p}' + \mathbf{q})\delta(\mathbf{q} - \mathbf{p}' + \mathbf{p})\delta(\omega - \omega_2 + \Omega)$$
$$\delta(\Omega - \omega_2 + \omega)g_0(\mathbf{k}, \omega)g_0(\mathbf{p}', \omega_2)\Gamma_{\alpha\phi}(\mathbf{p}, \mathbf{k}', \omega_1, \omega')\delta_{\psi\delta}\delta_{\beta\gamma}p_k p_l' M_{\alpha\beta\gamma\delta}^{kl}(\mathbf{q}, \Omega),$$

where the terms on the RHS are the zero-order, I_α and I_δ contributions respectively. The calculation goes through in much the same way as eqs. (36) - (37), yielding

$$I_\alpha = -\frac{i}{2}\int d\mathbf{q} d\Omega \ g_0(\mathbf{k}, \omega)g_0(\mathbf{k} - \mathbf{q}, \omega - \Omega)k_l(\mathbf{k} - \mathbf{q})_k M_{\alpha\psi\gamma\alpha}^{kl}(\mathbf{q}, \Omega)\Gamma_{\gamma\phi}(\mathbf{k}, \mathbf{k}', \omega, \omega'). \tag{E.2}$$

$$I_\delta = -\frac{i}{2}\int d\mathbf{q} d\Omega \ g_0(\mathbf{k}, \omega)g_0(\mathbf{k} + \mathbf{q}, \omega + \Omega)\left(k^2 - \frac{1}{q^2}(\mathbf{k} \cdot \mathbf{q})^2\right)\gamma(\mathbf{q}, \Omega)\Gamma_{\psi\phi}(\mathbf{k}, \mathbf{k}', \omega, \omega'). \tag{E.3}$$
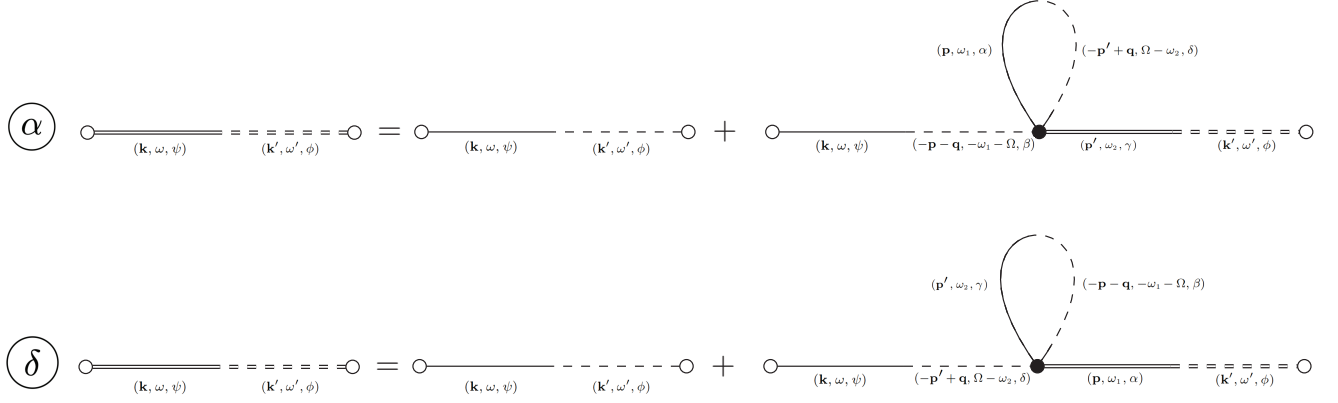
FIG. 6. Diagrammatic illustration of the expansion for the quantity $\langle \mathbf{A}(\mathbf{k})\tilde{\mathbf{A}}(\mathbf{k}')\rangle$. Note that the joined pairs of double lines contribute an exact propagator Γ, rather than a zero order propagator g_0. Only two diagrams, I_α and I_δ, contribute, as in section IV B.

Equation (E.1) may then be written as

$$g_0(\mathbf{k},\omega)\delta(\mathbf{k}+\mathbf{k}')\delta(\omega+\omega')\delta_{\psi\phi} = \Gamma_{\psi\phi}(\mathbf{k},\mathbf{k}',\omega,\omega')$$
$$\left[1+\int d\!\!\!/\mathbf{q}d\!\!\!/\Omega\;\frac{\gamma(\mathbf{q},\Omega)}{2}g_0(\mathbf{k},\omega)\left(g_0(\mathbf{k}-\mathbf{q},\omega-\Omega)+g_0(\mathbf{k}+\mathbf{q},\omega+\Omega)\right)\left(k^2-\frac{(\mathbf{k}\cdot\mathbf{q})^2}{q^2}\right)\right], \quad \text{(E.4)}$$

where the $\Gamma_{\psi\phi}$ terms have been collected on the LHS. It follows that

$$\Gamma_{\psi\phi}(\mathbf{k},\mathbf{k}',\omega,\omega') = \frac{g_0(\mathbf{k},\omega)\delta(\mathbf{k}+\mathbf{k}')\delta(\omega+\omega')\delta_{\psi\phi}}{1+g_0(\mathbf{k},\omega)\Xi(\mathbf{k},\omega)}, \quad \text{(E.5)}$$

where

$$\Xi(\mathbf{k},\omega) = \frac{1}{2}\int d\!\!\!/\mathbf{q}d\!\!\!/\Omega\;\gamma(\mathbf{q},\Omega)\left[g_0(\mathbf{k}-\mathbf{q},\omega-\Omega)+g_0(\mathbf{k}+\mathbf{q},\omega+\Omega)\right]\left(k^2-\frac{1}{q^2}(\mathbf{k}\cdot\mathbf{q})^2\right). \quad \text{(E.6)}$$

Equation (E.5) enables us to compute the magnetic vector potential's Green function to all orders in the loop integral. To obtain the magnetic field's Green function we make use of (31) again, noting that this time it accounts for the contribution of the loop diagrams to all orders

$$\begin{aligned}\mathcal{G}_{\alpha\beta}(\mathbf{k},\mathbf{k}',\omega,\omega') &= \frac{(2\pi)^3}{k^2}\delta(\mathbf{k}+\mathbf{k}')\delta(\omega+\omega')\varepsilon_{\beta n\phi}\varepsilon_{\alpha l\psi}k_n k_l\left(\delta_{\psi\phi}\frac{g_0(\mathbf{k},\omega)}{1+g_0(\mathbf{k},\omega)\Xi(\mathbf{k},\omega)}\right)\\ &= \frac{(2\pi)^3\delta(\mathbf{k}+\mathbf{k}')\delta(\omega+\omega')\sigma_{\alpha\beta}(\mathbf{k})\delta_{\psi\phi}}{g_0(\mathbf{k},\omega)^{-1}+\Xi(\mathbf{k},\omega)}.\end{aligned} \quad \text{(E.7)}$$

[1] A. J. Biggin, M. J. de Wit, C. G. Langereis, T. E. Zegers, S. Voûte, M. J. Dekkers, and K. Drost, Palaeomagnetism of archaean rocks of the onverwacht group, barberton greenstone belt (southern africa): Evidence for a stable and potentially reversing geomagnetic field at ca. 3.5 ga, Earth and Planetary Science Letters **302**, 314 (2011).

[2] C. S. Borlina, B. P. Weiss, E. A. Lima, F. Tang, R. J. Taylor, J. F. Einsle, R. J. Harrison, R. R. Fu, E. A. Bell, E. W. Alexander, et al., Reevaluating the evidence for a hadean-eoarchean dynamo, Science advances **6**, eaav9634 (2020).

[3] N. Gillet, D. Jault, E. Canet, and A. Fournier, Fast torsional waves and strong magnetic field within the earth's core, Nature **465**, 74 (2010).

[4] J. Aubert and C. C. Finlay, Geomagnetic jerks and rapid hydromagnetic waves focusing at earth's core surface, Nature Geoscience **12**, 393 (2019).

[5] B. Buffett and H. Matsui, Equatorially trapped waves in earth's core, Geophysical Journal International **218**, 1210 (2019).

[6] R. Chi-Durán, M. S. Avery, and B. A. Buffett, Signatures of high-latitude waves in observations of geomagnetic acceleration, Geophysical Research Letters **48**, e2021GL094692 (2021).

[7] N. Gillet, F. Gerick, D. Jault, T. Schwaiger, J. Aubert, and M. Istas, Satellite magnetic data reveal interannual waves in earth's core, Proceedings of the National Academy of Sciences **119**, e2115258119 (2022).

[8] L. Ziegler, C. Constable, C. Johnson, and L. Tauxe, Padm2m: a penalized maximum likelihood model of the 0–2 ma palaeomagnetic axial dipole moment, Geophysical Journal International **184**, 1069 (2011).

[9] M. Korte, C. Constable, F. Donadini, and R. Holme, Reconstructing the holocene geomagnetic field, Earth and Planetary Science Letters **312**, 497 (2011).

[10] S. Panovska, M. Korte, C. Finlay, and C. Constable, Limitations in paleomagnetic data and modelling techniques and their impact on holocene geomagnetic field models, Geophysical Journal International **202**, 402 (2015).

[11] C. A. Jones, Planetary magnetic fields and fluid dynamos, Annual Review of Fluid Mechanics **43**, 583 (2011).

[12] W. Kuang and B. F. Chao, Topographic core-mantle coupling in geodynamo modeling, Geophysical research letters **28**, 1871 (2001).

[13] P. A. Davidson, *Turbulence: an introduction for scientists and engineers* (Oxford university press, 2015).

[14] B. A. Buffett, L. Ziegler, and C. G. Constable, A stochastic model for palaeomagnetic field variations, Geophysical Journal International **195**, 86 (2013).

[15] Y. Guyodo and J. Valet, Global changes in geomagnetic intensity during the past 800 thousand years, Nature **399**, 249 (1999).

[16] J.-P. Valet, L. Meynadier, and Y. Guyodo, Geomagnetic dipole strength and reversal rate over the past two million years, Nature **435**, 802 (2005).

[17] D. G. Meduri and J. Wicht, A simple stochastic model for dipole moment fluctuations in numerical dynamo simulations, Frontiers in Earth Science **4**, 38 (2016).

[18] B. Buffett and A. Puranam, Constructing stochastic models for dipole fluctuations from paleomagnetic observations, Physics of the Earth and Planetary Interiors **272**, 68 (2017).

[19] M. Morzfeld and B. A. Buffett, A comprehensive model for the kyr and myr timescales of earth's axial magnetic dipole field, Nonlinear Processes in Geophysics **26**, 123 (2019).

[20] W. Davis and B. Buffett, Inferring core processes using stochastic models of the geodynamo, Geophysical Journal International **228**, 1478 (2022).

[21] P. Hoyng, M. Ossendrijver, and D. Schmitt, The geodynamo as a bistable oscillator, Geophysical & Astrophysical Fluid Dynamics **94**, 263 (2001).

[22] C. R. Scullard and B. A. Buffett, Probabilistic structure of the geodynamo, Physical Review E **98**, 063112 (2018).

[23] A. Kazantsev, Enhancement of a magnetic field by a conducting fluid, Sov. Phys. JETP **26**, 1031 (1968).

[24] R. H. Kraichnan, Diffusion of passive-scalar and magnetic fields by helical turbulence, Journal of Fluid Mechanics **77**, 753 (1976).

[25] G. Falkovich, K. Gawędzki, and M. Vergassola, Particles and fields in fluid turbulence, Reviews of modern Physics **73**, 913 (2001).

[26] A. Brandenburg and K. Subramanian, Astrophysical magnetic fields and nonlinear dynamo theory, Physics Reports **417**, 1 (2005).

[27] K. Subramanian, The origin, evolution and signatures of primordial magnetic fields, Reports on Progress in Physics **79**, 076901 (2016).

[28] H. Gomi and K. Hirose, Electrical resistivity and thermal conductivity of hcp fe–ni alloys under high pressure: Implications for thermal convection in the earth's core, Physics of the Earth and Planetary Interiors **247**, 2 (2015).

[29] Q. Williams, The thermal conductivity of earth's core: A key geophysical parameter's constraints and uncertainties, Annual Review of Earth and Planetary Sciences **46**, 47 (2018).

[30] O. Barrois, M. Hammer, C. Finlay, Y. Martin, and N. Gillet, Assimilation of ground and satellite magnetic measurements: inference of core surface magnetic and velocity field changes, Geophysical Journal International **215**, 695 (2018).

[31] C. C. Finlay, C. Kloss, N. Olsen, M. D. Hammer, L. Tøffner-Clausen, A. Grayver, and A. Kuvshinov, The chaos-7 geomagnetic field model and observed changes in the south atlantic anomaly, Earth, Planets and Space **72**, 1 (2020).

[32] H. K. Moffatt, *Field generation in electrically conducting fluids*, 2 (Cambridge University Press, 1978).

[33] R. H. Kraichnan, Small-scale structure of a scalar field convected by turbulence, The Physics of Fluids **11**, 945 (1968).

[34] S. Vainshtein, Dynamo of small-scale fields, Zhurnal Eksperimentalnoi i Teoreticheskoi Fiziki **79**, 2175 (1980).

[35] E. Balkovsky and A. Fouxon, Universal long-time properties of lagrangian statistics in the batchelor regime and their application to the passive scalar problem, Physical Review E **60**, 4164 (1999).

[36] A. A. Schekochihin, S. A. Boldyrev, and R. M. Kulsrud, Spectra and growth rates of fluctuating magnetic fields in the kinematic dynamo theory with large magnetic prandtl numbers, The Astrophysical Journal **567**, 828 (2002).

[37] D. Sokoloff and N. Yokoi, Path integrals for mean-field equations in nonlinear dynamos, Journal of Plasma Physics **84**, 735840307 (2018).

[38] P. C. Martin, E. Siggia, and H. Rose, Statistical dynamics of classical systems, Physical Review A **8**, 423 (1973).

[39] H.-K. Janssen, On a lagrangean for classical field dynamics and renormalization group calculations of dynamical critical properties, Zeitschrift für Physik B Condensed Matter **23**, 377 (1976).

[40] C. De Dominicis, A lagrangian version of halperin-hohenberg-ma models for the dynamics of critical phenomena, Lettere al Nuovo Cimento (1971-1985) **12**, 567 (1975).

[41] D. Forster, D. R. Nelson, and M. J. Stephen, Large-distance and long-time properties of a randomly stirred fluid, Phys. Rev. A **16**, 732 (1977).

[42] N. Yokoi, Turbulence, transport and reconnection, in *Topics in Magnetohydrodynamic Topology, Reconnection and Stability Theory*, edited by D. MacTaggart and A. Hillier (Springer International Publishing, Cham, 2020) pp. 177–265.

[43] P. Hoyng, D. Schmitt, and M. Ossendrijver, A theoretical analysis of the observed variability of the geomagnetic dipole field, Physics of the Earth and Planetary Interiors **130**, 143 (2002).

[44] M. Sadhasivan and C. Constable, A new power spectrum and stochastic representation for the geomagnetic axial dipole, Geophysical Journal International **231**, 15 (2022).

[45] B. Buffett, M. Avery, and W. Davis, A physical interpretation of asymmetric growth and decay of the geomagnetic dipole moment, Geochemistry, Geophysics, Geosystems **23**, e2021GC010239 (2022).

[46] D. Holdenried-Chernoff and B. Buffett, Evidence for turbulent magnetic diffusion in earth's core, Geochemistry, Geophysics, Geosystems , e2022GC010672 (2022).

[47] J. Cardy, G. Falkovich, and K. Gawędzki, *Non-equilibrium statistical mechanics and turbulence*, 355 (Cambridge University Press, 2008).

[48] A. Altland and B. D. Simons, *Condensed matter field theory* (Cambridge university press, 2010).

[49] M. Peskin and D. Schroeder, *An Introduction To Quantum Field Theory (Frontiers in Physics)(Boulder, CO* (Westview Press, 1995).

[50] T. Lancaster and S. J. Blundell, *Quantum field theory for the gifted amateur* (OUP Oxford, 2014).

[51] M. Steenbeck, F. Krause, and K.-H. Rädler, Berechnung der mittleren lorentz-feldstärke für ein elektrisch leitendes medium in turbulenter, durch coriolis-kräfte beeinflußter bewegung, Zeitschrift für Naturforschung A **21**, 369 (1966).

[52] U. R. Christensen and A. Tilgner, Power requirement of the geodynamo from ohmic losses in numerical and laboratory dynamos, Nature **429**, 169 (2004).

[53] F. J. Dyson, The s matrix in quantum electrodynamics, Physical Review **75**, 1736 (1949).

[54] L. D. Faddeev and V. N. Popov, Feynman diagrams for the yang-mills field, Physics Letters B **25**, 29 (1967).